

RESEARCH ARTICLE

10.1002/2015GC005911

Key Points:

- The isotope geochemistry of the western Pacific Plate slab is reported
- The Pacific Plate originated from both Indian and Pacific mantle
- The Indian-Pacific mantle boundary has been stationary in the western Pacific

Supporting Information:

- Supporting Information S1
- Data Set S1

Correspondence to:

T. Miyazaki,
tmiazaki@jamstec.go.jp

Citation:

Miyazaki, T., et al. (2015), Missing western half of the Pacific Plate: Geochemical nature of the Izanagi-Pacific Ridge interaction with a stationary boundary between the Indian and Pacific mantles, *Geochem. Geophys. Geosyst.*, 16, 3309–3332, doi:10.1002/2015GC005911.

Received 13 MAY 2015

Accepted 5 SEP 2015

Accepted article online 14 SEP 2015

Published online 30 SEP 2015

Missing western half of the Pacific Plate: Geochemical nature of the Izanagi-Pacific Ridge interaction with a stationary boundary between the Indian and Pacific mantles

Takashi Miyazaki¹, Jun-Ichi Kimura¹, Ryoko Senda¹, Bogdan S. Vaglarov¹, Qing Chang¹, Toshiro Takahashi², Yuka Hirahara³, Folkmar Hauff⁴, Yasutaka Hayasaka⁵, Sakae Sano⁶, Gen Shimoda⁷, Osamu Ishizuka⁷, Hiroshi Kawabata⁸, Naoto Hirano⁹, Shiki Machida¹⁰, Teruaki Ishii¹¹, Kenichiro Tani¹², and Takeyoshi Yoshida¹³

¹Department of Solid Earth Geochemistry, Japan Agency for Marine-Earth Science and Technology, Yokosuka, Japan,

²Department of Geology, Niigata University, Niigata, Japan, ³Chiba Institute of Technology, Chiba, Japan, ⁴Helmholtz

Centre for Ocean Research, GEOMAR, Kiel, Germany, ⁵Department of Earth and Planetary Systems Science, Graduate

School of Science, Hiroshima University, Higashi-Hiroshima, Japan, ⁶Earth Science Laboratory, Faculty of Education, Ehime

University, Matsuyama, Japan, ⁷Geological Survey of Japan, AIST, Tsukuba, Japan, ⁸Research and Education Faculty,

Multidisciplinary Science Cluster, Interdisciplinary Science Unit, Kochi University, Kochi, Japan, ⁹Center for Northeast

Asian Studies, Tohoku University, Sendai, Japan, ¹⁰Department of Resources and Environmental Engineering, Waseda

University, Tokyo, Japan, ¹¹Fukuda Geological Institute, Tokyo, Japan, ¹²Division of Mineral Sciences, National Museum

of Nature and Science, Tsukuba, Japan, ¹³Department of Earth Sciences, Graduate School of Science, Tohoku University,

Sendai, Japan

Abstract The source mantle of the basaltic ocean crust on the western half of the Pacific Plate was examined using Pb-Nd-Hf isotopes. The results showed that the subducted Izanagi-Pacific Ridge (IPR) formed from both Pacific (180–~80 Ma) and Indian (~80–70 Ma) mantles. The western Pacific Plate becomes younger westward and is thought to have formed from the IPR. The ridge was subducted along the Kurile-Japan-Nankai-Ryukyu (KJNR) Trench at 60–55 Ma and leading edge of the Pacific Plate is currently stagnated in the mantle transition zone. Conversely, the entire eastern half of the Pacific Plate, formed from isotopically distinct Pacific mantle along the East Pacific Rise and the Juan de Fuca Ridge, largely remains on the seafloor. The subducted IPR is inaccessible; therefore, questions regarding which mantle might be responsible for the formation of the western half of the Pacific Plate remain controversial. Knowing the source of the IPR basalts provides insight into the Indian-Pacific mantle boundary before the Cenozoic. Isotopic compositions of the basalts from borehole cores (165–130 Ma) in the western Pacific show that the surface oceanic crust is of Pacific mantle origin. However, the accreted ocean floor basalts (~80–70 Ma) in the accretionary prism along the KJNR Trench have Indian mantle signatures. This indicates the younger western Pacific Plate of IPR origin formed partly from Indian mantle and that the Indian-Pacific mantle boundary has been stationary in the western Pacific at least since the Cretaceous.

1. Introduction

1.1. Global-Scale Indian-Pacific Mantle Boundary

The heterogeneous nature of the mantle remains a major topic of debate, and heterogeneities ranging from centimeter to hemispheric scale have been proposed [Allegre and Turcotte, 1986; Davies, 2009; Hart, 1984; Hofmann, 2003; Iwamori et al., 2010; Stixrude and Lithgow-Bergelloni, 2012]. The most distinctive feature in global-scale mantle heterogeneity is the Indian and Pacific mantle domains. This characteristic is related to the identification of global Pb isotopic signatures found in the Southern Hemisphere (DUPAL anomaly) [Dupré and Allegre, 1983; Hanan and Graham, 1996; Hart, 1984] that were later revised according the growing isotope database from mid-ocean ridge basalts (MORBs) using Pb [Mahoney et al., 1998] and Nd-Hf isotopes [Chauvel and Blichert-Toft, 2001; Pearce et al., 1999]. Although the latest compilation of MORB data shows a diffused Indian-Pacific mantle boundary [Class and Lehnert, 2012], radiogenic ²⁰⁷Pb and ²⁰⁸Pb at a given ²⁰⁶Pb isotope composition and radiogenic Hf at a given Nd isotope composition in the Indian mantle still distinguishes the two large mantle domains, particularly the “enriched” Indian mantle.

In this sense, the enriched Indian mantle is widely distributed within the Indian and Atlantic oceans, whereas the Pacific Ocean is underlain only by “depleted” Pacific mantle [Nebel *et al.*, 2007], forming the East-West mantle hemispheres [Iwamori *et al.*, 2010].

The western Pacific is the hemispheric boundary of the Indian-Pacific mantle domain, which has been examined by various combinations of Pb-Nd-Hf isotope systems such as the Kurile-Japan-Izu-Mariana Trench [Flower *et al.*, 2001; Hickey-Vargas *et al.*, 1995, 2006; Hirahara *et al.*, 2015; Kimura and Yoshida, 2006; Kimura and Nakajima, 2014; Kimura *et al.*, 2010; Martynov *et al.*, 2012; Park *et al.*, 2006; Savov *et al.*, 2006; Woodhead *et al.*, 2012], Vitiaz-Tonga Trench [Pearce *et al.*, 2007], and Australia-Antarctica Discordance [Hanan *et al.*, 2004; Kempton *et al.*, 2002; Klein *et al.*, 1988; Pyle *et al.*, 1995]. The current global boundary of the two mantle domains is expected to be located along the N-S-trending Kurile-Japan-Izu and Mariana-Vitiaz-Tonga trenches and Australia-Antarctica Discordance, rimming the western margins of the Pacific Ocean basin [Machida *et al.*, 2009; Nebel *et al.*, 2007; Pearce *et al.*, 1999] (Figure 1a). Accordingly, the consensus on the boundary of the Indian-Pacific mantle in the present-day western Pacific relates to the surface of the Pacific Plate slab subducting beneath the North American, Eurasian, Philippine Sea, and Indo-Australian plates [Machida *et al.*, 2009; Nebel *et al.*, 2007; Pearce *et al.*, 1999], although the detailed position of the boundary, e.g., the Caroline basin, differs slightly among researchers.

This global-scale mantle domain is thought to have been present since the Permian along the subduction zones at the eastern margins of the Gondwana supercontinent [Müller *et al.*, 2008; Nebel *et al.*, 2007] (Figure 2). Pacific Plate subduction continued during the Cretaceous, when the Gondwana continent broke up, and after the re-organization of the upper plates with the northward migration of the Australian continent and formation of the Philippine Sea Plate [Hall, 2002; Müller *et al.*, 2008]. It appears that the location of the subduction zone, where various Panthalassa plates including the present-day Pacific Plate subducted, has been the boundary between the Indian-Pacific mantle, bordering the sub-Gondwana “continental” and the sub-Pacific “oceanic” upper mantle for >140 Myr [Flower *et al.*, 2001; Hickey-Vargas *et al.*, 1995; Machida *et al.*, 2009; Mahoney *et al.*, 1998; Pearce *et al.*, 1999].

Debate continues on the ancient location of the mantle domain boundary. This topic is related to the onset of the subduction of the Pacific Plate beneath the Philippine Sea plate, which occurred at ~52 Ma in the Izu-Bonin-Mariana arc. The onset of subduction along the eastern margins of the Eurasian and Philippine Sea plates led to the Pacific Plate slab intruded into the Indian mantle. Thus, the surface of the Pacific Plate slab became the boundary between the Indian-Pacific mantle domains at that time [Pearce *et al.*, 1999]. However, the Indian-Pacific mantle boundary could have been “beneath the presubducted Pacific Plate” prior to this event [Pearce *et al.*, 1999]. If true, then before ~52 Ma, the Indian-Pacific mantle boundary would have been located in the Equatorial western Pacific Ocean basin, contradicting the boundary model of the older Gondwana margins. An alternative model is that the mantle beneath the plate suture was influenced by local Manus plume activity, which initiated the subduction and from which the enriched (Indian mantle-like) mantle component was introduced into the infant arc magmas [Macpherson and Hall, 2001].

1.2. Mantle Beneath the Pacific Plate

Recently, the previous consensus regarding the Indian mantle provenance of the wedge mantle above the Pacific Plate in the Kurile-Japan-Izu-Mariana arc (Figure 1) was challenged based on analysis of the slab flux in the lavas from these arcs [Straub *et al.*, 2009, 2015]. Straub *et al.* [2009] showed that relatively elevated $^{207}\text{Pb}/^{204}\text{Pb}$ and $^{208}\text{Pb}/^{204}\text{Pb}$ in the arc lavas are spatially limited in the area in which the age of the subducted Pacific Plate slab is younger than 125 Ma (Figure 1). Straub *et al.* [2009] reported that the radiogenic Pb was largely from the altered oceanic crust (AOC) of the Pacific Plate, and they proposed that the Pacific Plate younger than ~125 Ma was generated from the previously subducted Izanagi-Pacific Ridge (IPR) [Nakanishi *et al.*, 1989], which produced MORBs of Indian mantle provenance (Indian-type MORB or AOC) as young as 125 Ma. This proposal is contrary to previous models that relied on Pb-Sr-Nd isotopic geochemistry of the arc lavas to determine the provenance of the Indian mantle wedge [Flower *et al.*, 2001; Hickey-Vargas *et al.*, 1995; Kimura and Yoshida, 2006; Kimura and Nakajima, 2014; Kimura *et al.*, 2010; Martynov *et al.*, 2012; Pearce *et al.*, 1999].

If the interpretation of Straub *et al.* [2009] is correct, the upper mantle beneath the younger western Pacific Plate of 70–125 Ma might be Indian mantle because the IPR Plate boundary subducted along the Kurile-Japan-Nankai-Ryukyu Trench at 60–55 Ma [Kiminami *et al.*, 1994; Müller *et al.*, 2008; Seton *et al.*, 2012, 2015;

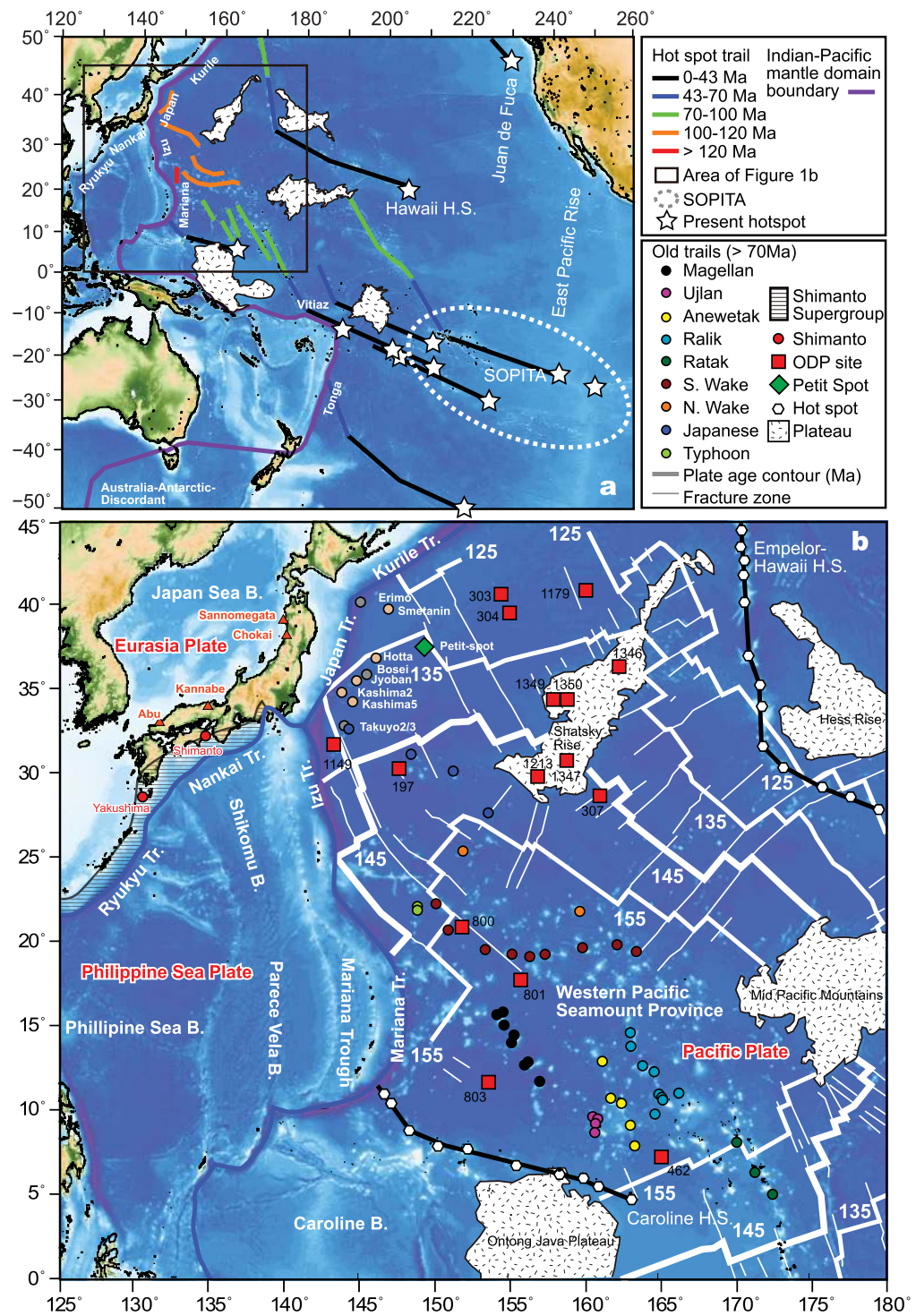


Figure 1. Map showing the Indian-Pacific mantle domain boundary, hot spot tracks, ridges, and subduction zones in the (a) Pacific and (b) western Pacific. Hot spot tracks, rises, and plateaus in Figure 1a are from *Condie* [2001]. Locations of the MORB and OIB samples used in this study are shown in Figure 1b. Borehole location data were obtained from the IODP web site at <http://www.iodp.org/borehole-map>. Thick white lines with numbers show ages of the Pacific plate, and thin lines show transform faults [*Nakanishi et al.*, 1989]. The SOPITA hot spot trails in Figures 1a and 1b are from *Koppers et al.* [2003]. Tr: trench; B: basin; HS: hotspot.

Whittaker et al., 2007] and the western leading edge of the Pacific Plate segment is believed to be currently stagnated in the mantle transition zone [*Fukao et al.*, 1992; *Sakuyama et al.*, 2013; *Seton et al.*, 2015] (Figure 3). Following the models of *Straub et al.* [2009, 2015], the Pacific-Indian mantle domain boundary in

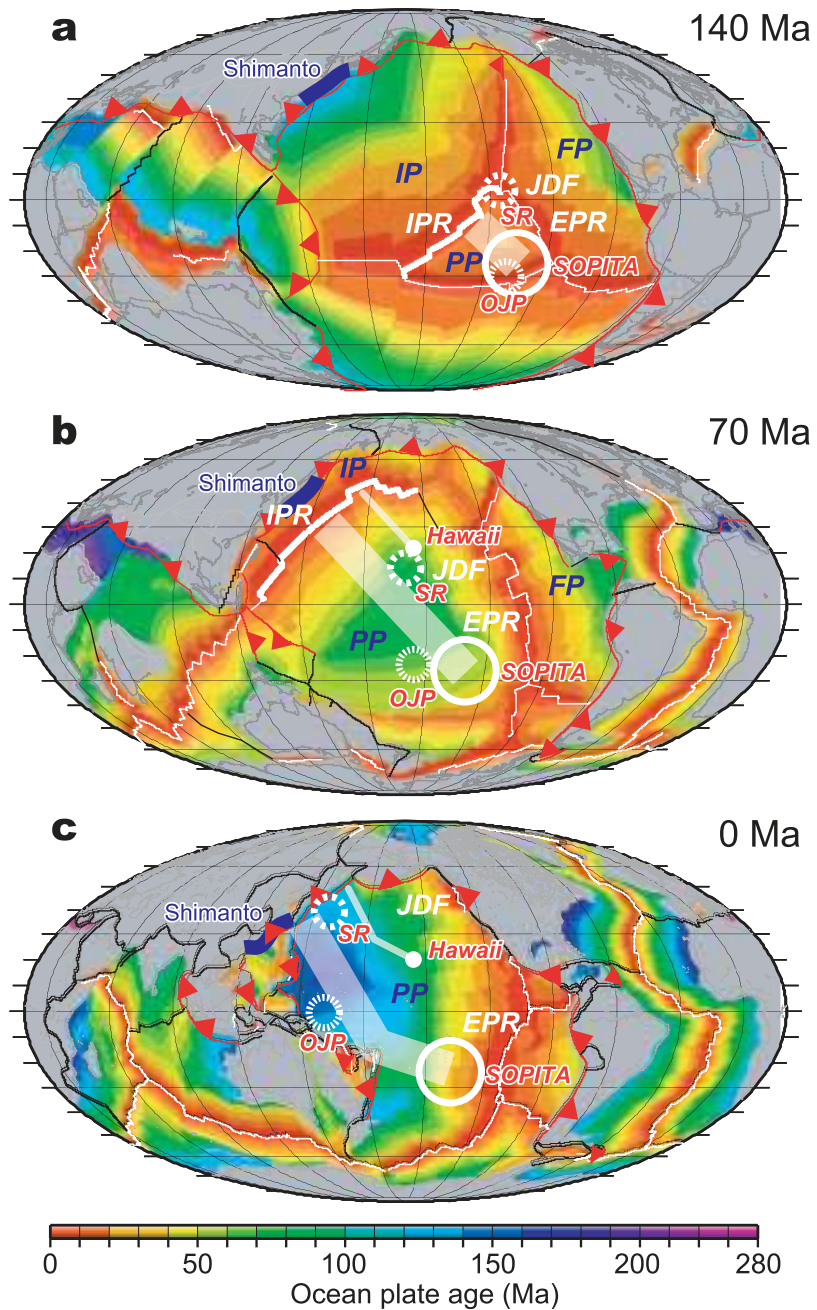


Figure 2. Paleogeographic map showing reconstruction of the Pacific Plate development. Figures were adopted from the literature [Müller *et al.*, 2008] and modified by the authors. IP: Izanagi Plate; FP: Farallon Plate; PP: Pacific Plate; IPR: Izanagi Pacific Ridge; JDF: Juan de Fuca Ridge; EPR: East Pacific Rise; SOPITA: South Pacific Thermal and Isotopic Anomaly; OJP: Ontong Java Plateau; SR: Shatsky Rise; Hawaii: Hawaii hot spot. Thick and thin white bands show SOPITA and Hawaii hotspot tracks, respectively. Red triangles show subduction zones, and thin white lines show spreading ridges. Thick dark blue line: location of the Shimanto accretionary prism through time.

the upper mantle should be located to the east of the Kurile-Japan-Nankai-Ryukyu Trench (Figure 3b), rather than at the trench itself (Figure 3a) as interpreted in other models [Flower *et al.*, 2001; Nebel *et al.*, 2007; Pearce *et al.*, 1999].

More recently, Straub *et al.* [2015] further extended the same analysis to the temporal and spatial variations of the lavas in the Izu and Mariana arcs. While the latest model confirmed the first proposal it also raised further questions. On the basis of Pb isotope systematics, they suggested that the Izu arc was influenced by the Pacific-type AOC from 52 to 42 Ma, followed by the Indian-type AOC from 42 to 0 Ma. Moreover, they

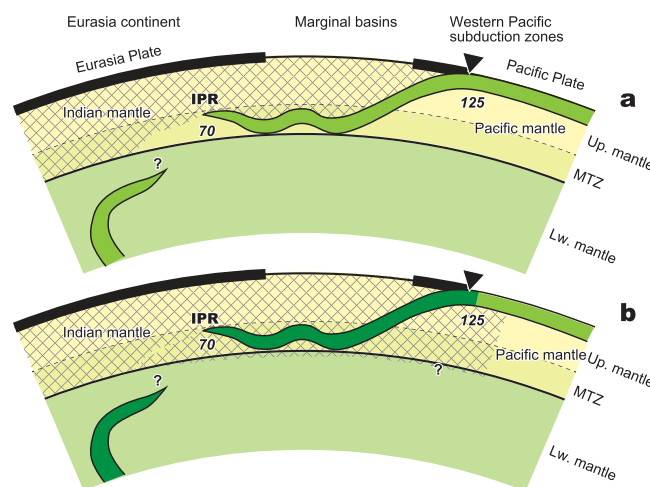


Figure 3. Schematics showing two models of the distribution of the Indian (hatching) and Pacific mantle domains in the upper mantle and uppermost lower mantle. Up: upper; Lw: lower; MTZ: mantle transition zone. Location of the sunken Izanagi Plate may be deeper according to the geodynamic model [Seton *et al.*, 2015].

(2) the Indian-Pacific mantle boundary was located beneath the western Pacific basin prior to the subduction of the IPR (Figures 2 and 3b). Therefore, the provenance of the mantle beneath the Pacific Plate, subduction zones, and marginal basins in the western Pacific is fundamental to understanding the arc-back arc magmatism and regional tectonics. The relationship of the Indian-Pacific mantle boundary in the upper mantle and in the mantle transition zone is also an important constraint to the mantle convection associated with a stagnant Pacific Plate slab in the mantle transition zone beneath Eurasia [Zhao *et al.*, 2009].

In this paper, we analyze trace elements and the Sr-Nd-Hf-Pb isotope compositions in the ocean floor basalts collected from the western Pacific (167–129 Ma), accreted Cretaceous ocean floor basalts in the Japanese accretionary prism (~80–70 Ma), and old (~118 Ma) ocean island basalts (OIBs) and young (~6 Ma) petit-spot basalts erupted on the western margins of the ~140 Myr-old Pacific Plate. On the basis of the new data and existing geochemical data, we discuss the origin of the Pacific Plate oceanic crust generated from the IPR and the location of the Indian-Pacific mantle boundary in the Cenozoic western Pacific. Furthermore, the nature of mantle heterogeneity within the region is examined to address the two aforementioned questions.

2. Geological and Geochemical Settings

Here we briefly summarize the important features of tectonics, geological settings, and geochemistry of the Pacific Plate reported in previous research.

2.1. Tectonic and Geological Settings

2.1.1. Plate Tectonics

The western Pacific Ocean is underlain by the oldest portion of the Pacific Plate, and the age of the plate becomes younger outward from the ~180 Myr-old Western Pacific Seamount Province (WPSP) to the ~120 Myr-old north-south Pacific rim and to the east up to the new seafloor being formed along the East Pacific Rise (EPR) and Juan de Fuca (JDF) Ridge (Figures 1 and 2) [Nakanishi *et al.*, 1989]. To the west, the Pacific Plate subducts beneath the Eurasian and Philippine Sea plates. The plate immediately before the subduction zone has an age range of 120–150 Ma along the present-day Kurile-Japan-Izu-Mariana Trench (Figures 1 and 2). The Philippine Sea Plate rapidly migrated to the north from the equatorial areas to its present position by 15 Ma [Hall, 2002; Kimura *et al.*, 2005]. Prior to this movement, the Pacific Plate subduction continued along the Kurile-Japan-Nankai-Ryukyu Trench forming the Shimanto Supergroup accretionary prism complex over a distance of >2500 km along the eastern margins of the Eurasian continent [Kimura *et al.*, 2005; Taira, 2001] (Figures 1 and 2). This accretionary prism formed continuously from >120 Ma to 60 Ma along the Kyushu-Japan-Nankai-Ryukyu subduction system [Taira, 2001]. During this time, the IPR

determined that the Mariana arc was influenced by the Pacific-type AOC from 51 to 24 Ma and the Indian-type AOC from 24 to 10 Ma. These hypotheses reflect the subduction of the IPR-sourced Pacific Plate formed in 100–90 Ma [Straub *et al.*, 2015]. They accepted the contribution of the arc mantle wedge of Indian mantle origin [Hickey-Vargas *et al.*, 1995, 2006; Park *et al.*, 2006; Savov *et al.*, 2006; Woodhead *et al.*, 2012]; thus, the mantle domain boundary issue deduced from AOC chemistry remains an open question.

1.3. Aim of This Paper

The proposal by Straub *et al.* [2009, 2015] raises two points of conjecture: (1) The trace of Indian mantle in the arc lavas is partly from the AOC and not entirely from the wedge mantle, and

subducted from 60 to 55 Ma [Müller *et al.*, 2008; Seton *et al.*, 2012, 2015; Whittaker *et al.*, 2007] (Figure 2b). Different models have been presented on the geometry of the IPR subduction; we used the model that implies that IPR subduction occurred almost parallel to the Kurile-Japan-Nankai-Ryukyu Trench [Müller *et al.*, 2008; Seton *et al.*, 2012, 2015; Whittaker *et al.*, 2007]. The IPR subduction may have occurred earlier considering the ages of the accreted MORBs of the Shimanto Supergroup (90–60 Ma) [Kiminami *et al.*, 1994], which may have affected the absolute location of the Indian-Pacific mantle boundary beneath the NW Pacific.

The eastern wing of the subducted IPR, specifically the Pacific Plate segment, is considered to be currently stagnant in the mantle transition zone 440–660 km deep beneath both the eastern Eurasian continent and the Japan Sea [Fukao *et al.*, 1992; Sakuyama *et al.*, 2013; Seton *et al.*, 2015]. Stagnation of the IPR Pacific slab might have caused the opening of the Japan Sea back-arc basin through slab rollback [Sdoliás and Müller, 2006]. The model suggests that the subducted, or missing, western half of the Pacific Plate was from the IPR and that it formed during the Cretaceous (125–60 Ma; Figures 2 and 3) because the entire lifetime of the IPR was 180–60 Ma, starting from the formation of the oldest Pacific Plate currently in the WPSP area [Müller *et al.*, 2008] (Figure 2a).

2.1.2. The Shimanto Accretionary Prism

The IPR ridge subduction left scraped-off oceanic basalts in the Shimanto Supergroup accretionary prism [Kiminami *et al.*, 1994]. These are now regarded as zeolite facies-type low metamorphic-grade greenstones [Asaki and Yoshida, 1998; Kiminami *et al.*, 1992] in the mudrocks and sandstones of the highly deformed Shimanto Supergroup. The Shimanto greenstones are mostly MORB-type, according to the major and trace element data determined by X-ray fluorescence spectrometry. The frequent occurrence of such greenstones in the Cretaceous (90–60 Ma) is attributed to IPR subduction [Kiminami *et al.*, 1994]. There is no evidence on back-arc basin subduction or arc magma genesis in this accretionary prism, and the Pacific Plate subduction is believed to have been ongoing since the Cretaceous [Kiminami *et al.*, 1992; Kiminami *et al.*, 1994; Müller *et al.*, 2008; Sdoliás and Müller, 2006; Taira, 2001] until the Shikoku Basin of the Philippine Sea Plate subduction occurred after ~15 Ma along the Nankai Trench. This theory is in contrast to that of continuous Pacific Plate subduction in the Kurile-Japan-Izu Trench [Kimura *et al.*, 2005; Taira, 2001].

A typical *in situ* ocean floor basalt exposure crops out in the Shimanto in Shikoku. The emplacement age was estimated to be ~70 Ma on the basis of the radiolarian fossil age from the host mudrocks; the former being stratigraphically continuous with the pillow lavas and the peperites [Asaki and Yoshida, 1998; Kiminami *et al.*, 1992] (Figure 1b). Similar greenstones are also found in the younger sedimentary rocks of the accretionary prism, such as at Yakushima Island, with a radiolarian fossil age of ~40 Ma showing the minimal age of the accreted greenstones [Saito *et al.*, 2007]. The Yakushima greenstones are unrelated to the ridge subduction but are representative of part of the scraped-off Pacific Plate from the IPR with a formation age of ~80 Ma, as shown through plate reconstruction in [Sdoliás and Müller [2006, Figure 5b] (Figure 1b).

2.2. Pb Isotope Geochemistry of Basalts From the Pacific Ocean

An existing comprehensive geochemical data set of Pb isotopes is relevant to the determination of the Indian-Pacific mantle boundary was used in this study. Figure 4 plots the time-corrected $^{208}\text{Pb}/^{204}\text{Pb}(t)$ and $^{206}\text{Pb}/^{204}\text{Pb}(t)$ ratios by using existing Pb isotope data based on the assumption that the MORBs and OIBs had similar Pb, Th, and U compositions as those of the normal (N)-MORBs and OIBs [Sun and McDonough, 1989], respectively. The use of the measured U-Th-Pb compositions in the samples did not alter the basic shapes of the plots. Their (t) ages were estimated from seafloor ages [Nakanishi *et al.*, 1989] for the MORBs, the measured Ar-Ar and estimated ages for the WPSP OIBs [Koppers *et al.*, 2003; Shimoda *et al.*, 2011], and the measured Ar-Ar ages for the petit-spot basalts [Hirano *et al.*, 2006]. The French Polynesian samples were not corrected because of their young ages [GEOROC, 2013; Stracke *et al.*, 2005]. Other reference lines and fields are shown at (t) = 0; their sources are listed in the caption for Figure 4. In section 2.2.1, we describe the Pb isotope compositions of the MORBs and OIBs on the Pacific Plate. The basalts from the Eurasian continent and marginal basins are examined in section 4 by using Nd-Hf isotopes.

2.2.1. MORBs

Previously reported geochemical analyses of the MORBs from the western Pacific Plate indicate Pacific mantle provenance. The time-corrected Pb isotopic compositions from DSDP Site 801 MORBs (~160 Ma; Figure 1b) in the WPSP are all Pacific, including the slightly high U/Pb mantle (HIMU)-like ($^{206}\text{Pb}/^{204}\text{Pb}(t) \approx 19$) volcanoclastics from Site 801; these are assumed to have been derived from the neighboring Cretaceous

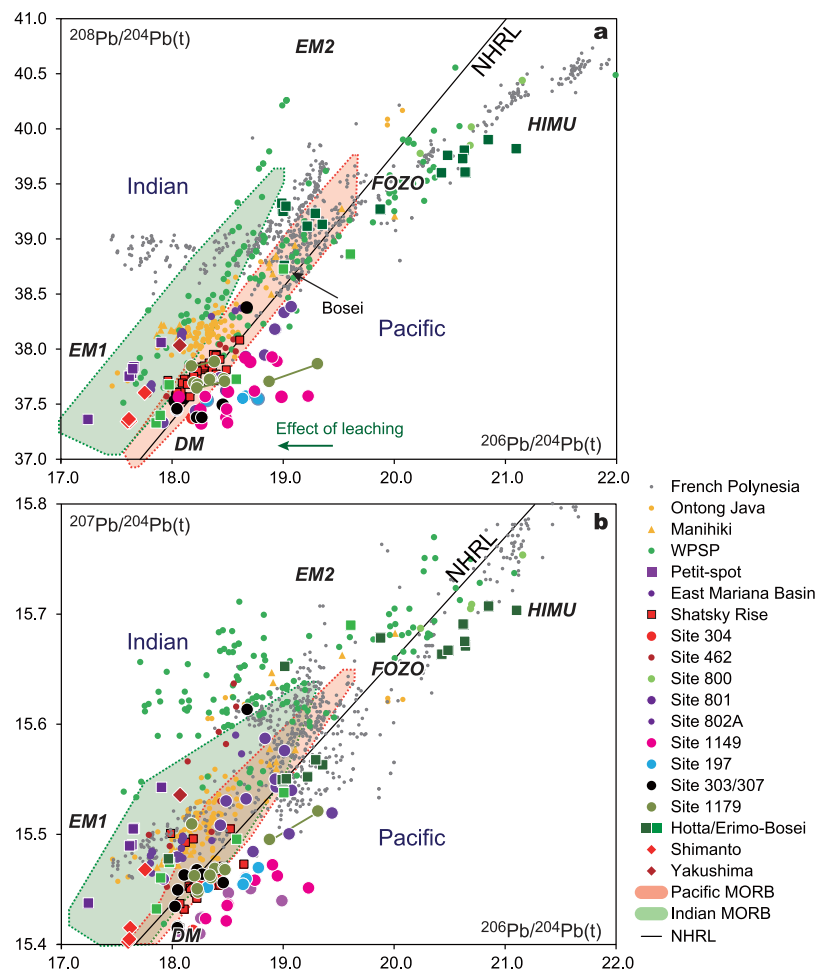


Figure 4. Time-corrected Pb isotopic compositions of the mid-ocean ridge basalts (MORBs) and ocean island basalts (OIBs) in the Pacific Ocean. Indian and Pacific MORB fields are (a) from Mahoney *et al.* [2005] and (b) from the data in Class and Lehnert [2012], confirmed by recent compilations of the Pacific and Indian-Atlantic MORBs [Class and Lehnert, 2012]. Locations of depleted mantle (DM), Focus Zone (FOZO), high U/Pb mantle (HIMU), Enriched Mantle 1 (EM1), and EM2 are from the literature [Stracke *et al.*, 2005]. Tie-lines for the Site 1179 samples were obtained from leaching experiments.

seamounts [Chauvel *et al.*, 2009] (Figure 4). The Pb isotopes of the ODP Site 1149 MORBs (~ 135 Ma; Figure 1b) from the front of the Izu arc indicate they are all from the Pacific mantle [Hauff *et al.*, 2003] (Figure 4). It is therefore reasonable that 130–160 Myr-old MORBs from the IPR have Pacific mantle provenance, as has been discussed previously and also by Straub *et al.* [2009]. The eastern half of the Pacific Plate is 0–180 Myr old, and the JDF Ridge and EPR are the present-day spreading ridges where the Pacific mantle geochemistry is defined [Hart, 1984; Machida *et al.*, 2009; Pearce *et al.*, 1999]. The Pacific MORB field is shown in Figure 4.

The oldest portion of the northeastern Pacific Plate, with JDF Ridge origin, is represented by the Shatsky Rise, which is large igneous province (LIP) in which a ridge-ridge-ridge (R-R-R) triple junction formed about 145–130 Ma [Nakanishi *et al.*, 1989] (Figures 1 and 2). The Shatsky Rise erupted from predominantly MORB-type basalt [Kimura and Kawabata, 2014; Sano *et al.*, 2012] with a Pacific mantle Pb isotopic signature [Heydolph *et al.*, 2014; Mahoney *et al.*, 2005]; basalts from Sites 1213, 1346, 1347, 1349, and 1350 in Figure 1b have the same Pb isotopic compositions as those shown in Figure 4. Therefore, the eastern half of the Pacific Plate, which originated from the IPR-EPR-JDF Pacific-Farallon plate boundary, including the 145–130 Ma Izanagi-Pacific-Farallon plate triple junction of the Shatsky Rise, commonly shared Pacific mantle geochemical affinity throughout its history. According to the existing data of the Pacific Plate MORBs, we did not observe signals of Indian mantle provenance in this plot.

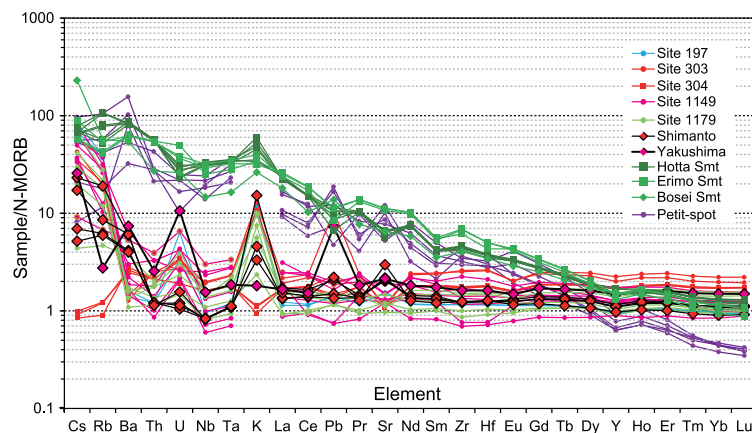


Figure 5. Normal mid-ocean ridge basalt (N-MORB) normalized multielement plots of the MORBs, ocean island basalts (OIBs), petit-spot basalts, and accreted Shimanto greenstones newly analyzed in this study. Normalization values are from *Pearce and Parkinson* [1993].

2.2.2. OIBs and Petit-Spot Basalts

In contrast to the MORBs in the Pacific, the geochemistry of the OIBs is highly variable, covering almost the entirety of mantle components of Enriched Mantle 1 (EM1) -EM2-HIMU-depleted mantle (DM) -Focus Zone (FOZO) [Hart *et al.*, 1992; Zindler and Hart, 1986] (Figure 4). Many South Pacific Isotopic and Thermal Anomaly (SOPITA) [Staudigel *et al.*, 1991] HIMU-FOZO-EM1-EM2 OIBs, particularly some Cretaceous WSPS lavas, possess radiogenic ^{207}Pb and ^{208}Pb [Koppers *et al.*, 2003] that reveal their similarity to the Indian mantle (Figure 4). Similarly, the Ontong-Java Plateau LIP basalts (Figures 1 and 2) overlap on the Indian mantle field in contrast to those of the Shatsky Rise (Figure 4). These plume-sourced OIBs in the Pacific have partial similarity with the Indian mantle [Farnetani and Hofmann, 2010; Ito and Mahoney, 2005; Kimura and Kawabata, 2015; Koppers *et al.*, 2003] (Figure 4).

The Cretaceous Hotta Seamount of ~ 118 Ma was active on the 136 Myr-old Pacific Plate that is currently near the Japan Trench (Figures 1 and 2). This activity is responsible for the oldest exposed SOPITA-influenced OIBs, which have the same age as the Magellan Seamounts and an HIMU component [Shimoda *et al.*, 2011] (Figure 4). OIBs from the nearby petit-spot volcanoes (~ 6 Ma) [Hirano *et al.*, 2006] (Figure 1) exhibit an EM1 isotope signature [Machida *et al.*, 2009] (Figure 4). This indicates that the shallow upper-mantle asthenosphere (~ 100 km) beneath the Pacific Plate may have been affected by the plume that locally shows Indian mantle-like composition, although their sizes appear to be small for petit-spot type [Machida *et al.*, 2009].

The petit-spot EM1 and Hotta Seamount HIMU OIBs may reflect a highly heterogeneous SOPITA plume-influenced mantle formed by underplating of plumes during ancient times (~ 118 Ma). The petit-spot basalts could be a product of the remelting of the EM1 source originating in plumes of the SOPITA area (see the overlap of the petit-spot basalts on the WSPS field in Figure 4). However, it is possible that the petit-spot basalts are nonplume in origin [Hirano *et al.*, 2006; Hofmann and Hart, 2007], and shallowly derived petit-spot volcanoes may have sampled Indian mantle (Figure 4).

Overall, the existing Pb isotopic data suggest that all MORBs of the Pacific Plate have Pacific mantle provenance, whereas part of the Pacific upper mantle and ocean crust has been modified by plumes in the SOPITA area [Koppers *et al.*, 2003; Shimoda *et al.*, 2011]. However, partial distribution of the Indian mantle beneath the Pacific Plate [Pearce *et al.*, 2007; Straub *et al.*, 2010, 2015] is another possibility. We examine the nature of the mantle beneath the Pacific Plate in a subsequent section.

3. Samples and Analytical

Here we describe the analyzed samples and analytical methods used in this study.

3.1. Analyzed Samples

To examine the trace elements and Nd-Hf-Pb isotopic compositions for the study of western Pacific Plate provenance, information was collected from the legacy core samples of the DSDP/ODP boreholes obtained

from the western Pacific, dredge samples of the OIBs from the Cretaceous seamounts on the western Pacific Plate, petit-spot basalt samples analyzed previously, and greenstones from the Shimanto Supergroup.

The DSDP and ODP have performed deep drilling in the western Pacific for many years and have recovered cores from oceanic floor basalts. The MORB samples analyzed here are from Sites 197 [Heezen *et al.*, 1973], 303 [Roger *et al.*, 1975a], 304 [Roger *et al.*, 1975b], and 1179 [Kanazawa *et al.*, 2001; Sano and Hayasaka, 2004]. These legacy core samples cover relatively young (~140–130 Ma) MORBs in the northwestern Pacific (Figure 1b) for which the Sr-Nd-Hf-Pb isotopic and trace element compositions were analyzed. We also analyzed the trace elements and Hf isotopic compositions for the same sample powder used in a previous study from Site 1149 to fulfill the Hf isotope data set [Hauff *et al.*, 2003]. Several sample powders were leached, and the results were compared with those from nonleached powders.

Dredge samples from the Hotta Seamounts analyzed previously [Shimoda *et al.*, 2011] were used in the present study, as were dredge samples from the Erimo and Bosei seamounts that erupted on the ~125 Myr-old Pacific Plate (Figure 1b). Existing isotope and trace element data were used together with the newly obtained Hf isotopic data for the Hotta Seamount OIBs. Full analyses were performed on the Erimo and Bosei OIB samples. Additionally, the petit-spot basalts [Machida *et al.*, 2009] were analyzed for Hf isotopes by using the same powders analyzed in the previous study after strong leaching. Trace element composition was analyzed for the nonleached powders.

In addition, we sampled the ~70 Ma MORB greenstones from the Shimanto Supergroup of the Mugi Formation in Shikoku [Asaki and Yoshida, 1998; Kiminami *et al.*, 1992] (Figure 1b). These basalts represent the IPR ridge MORBs that erupted at ~70 Ma [Asaki and Yoshida, 1998; Kiminami *et al.*, 1992]. For comparison, we also analyzed an accreted young Shimanto greenstone in a ~40 Ma mudrock from Yakushima Island [Saito *et al.*, 2007], which represents the IPR-derived Pacific Plate most likely ~80 Myr old in eruption age [Sdoliias and Müller, 2006]. Full data sets were obtained for these rocks. We analyzed the strongly leached powders for the isotopic measurements because interaction between the greenstone basalts and host mudrocks was clear, particularly in Shimanto as shown by the peperite and hydrothermal zeolite veins [Asaki and Yoshida, 1998; Kiminami *et al.*, 1992]. However, these portions in the samples were carefully discarded during the sampling.

3.2. Analytical Methods

All the analyses were conducted at Japan Agency for Marine-Earth Science and Technology (JAMSTEC). Trace element concentrations were measured by using digested powder samples without leaching through the use of an inductively coupled plasma mass spectrometer (ICP-MS; Agilent 7500ce; Agilent Technologies, Omaha, Neb., U.S.A.), following a previously reported method [Chang *et al.*, 2003]. Both the analytical reproducibility and precision for the rock samples were better than 5%. The same sample powders were analyzed to detect radiogenic isotopes. Part of the sample powders was further acid-leached following the method of McDonough and Chauvel [1991], except for some Shimanto greenstone samples, which were leached three times by using 6M of hot HCl for 2 h. The leached samples were also analyzed for trace elements in order to measure parent-daughter elemental ratios for the radiogenic isotopes because age consistency is better maintained between the elemental ratios and radiogenic isotopes in the residual mineral-leached powders [Hanyu *et al.*, 2011].

The analytical procedures for the isotopic ratios included chemical separation and mass spectrometry, following the methods reported previously for Sr, Nd, and Pb isotopes [Hirahara *et al.*, 2012; Miyazaki *et al.*, 2012; Takahashi *et al.*, 2009]. Isotopic ratios of Sr and Nd were determined by using a thermal ionization mass spectrometer (Triton TI; Thermo Fisher Scientific, Bremen, Germany), with fractionation correction by using $^{86}\text{Sr}/^{88}\text{Sr} = 0.1194$ and $^{146}\text{Nd}/^{144}\text{Nd} = 0.7219$, respectively. The value of SRM 987 measured during the analyses was $^{86}\text{Sr}/^{88}\text{Sr} = 0.710245 \pm 22$ (2 standard deviation (2 SD), $n = 13$) and that for JNdi-1 was $^{143}\text{Nd}/^{144}\text{Nd} = 0.512101 \pm 10$ (2 SD, $n = 11$).

The Pb isotopic ratios were determined by using a multiple collector (MC)-ICP-MS Neptune (Thermo Fisher Scientific, Bremen, Germany). Mass fractionation factors for Pb were corrected using TI as an external standard. Additional mass-dependent inter-element fractionations were corrected by applying a standard bracketing method using National Institute of Standards and Technology (NIST) standard reference material (SRM) 981 as a standard [Kimura *et al.*, 2006]. The $^{206}\text{Pb}/^{204}\text{Pb}$, $^{207}\text{Pb}/^{204}\text{Pb}$, and $^{208}\text{Pb}/^{204}\text{Pb}$ values of the

repeated measurements of NIST 981 were 16.9322 ± 11 , 15.4857 ± 14 , and 36.6810 ± 46 (2 SD, $n = 46$), respectively, and the Pb isotope data were obtained after normalization using the SRM 981 values to $^{206}\text{Pb}/^{204}\text{Pb} = 16.9416$, $^{207}\text{Pb}/^{204}\text{Pb} = 15.5000$, and $^{208}\text{Pb}/^{204}\text{Pb} = 36.7262$ [Baker et al., 2004].

Hf was separated by using the single-column method [Münker et al., 2001] if only the Hf isotope was analyzed or by the single-column method [Münker et al., 2001] after preliminary separation if cation ion-exchange resin was also used. The Hf isotope ratios were measured by using the Neptune Multi-collector (MC)-ICP-MS (Thermo Fisher Scientific, Bremen, Germany). Mass fractionation was determined from $^{179}\text{Hf}/^{177}\text{Hf}$, and the isotope ratios were normalized to $^{179}\text{Hf}/^{177}\text{Hf} = 0.7325$ by using an exponential law. The ^{173}Yb and ^{175}Lu peaks were monitored to correct for interference on the ^{176}Hf peak from ^{176}Yb and ^{176}Lu , which was usually negligible. Repeated measurements of the JMC475 yielded $^{176}\text{Hf}/^{177}\text{Hf} = 0.282144 \pm 4$ (2 SD, $n = 57$) during the analyses. The reported value of $^{176}\text{Hf}/^{177}\text{Hf}$ was further adjusted to JMC475 $^{176}\text{Hf}/^{177}\text{Hf} = 0.28216$. Total procedural blanks for Sr, Nd, Hf, and Pb were less than 37, 12, 40, and 44 pg, respectively.

The analytical results of the United States Geological Survey (USGS) rock standards BHVO-2, BCR-2 and those of the Geological Survey of Japan (GSJ) rock standard JB-2, measured in the course of this study, are shown in the supporting information Data Set S1, together with the data for the basalt samples. All showed excellent agreement with the preferred values in the GeoReM standard database [Jochum et al., 2005].

4. Results

In this section, we describe the trace elements and Pb-Nd-Hf isotope characteristics of the analyzed samples and compare them with the existing data set. Although the Sr isotope ratios were analyzed, they were affected severely by seawater alteration and possible mudrock contamination; therefore, detailed description of the Sr isotope results was disregarded.

4.1. Leaching Tests

We examined the effect of seafloor alteration by analyzing the Nd isotope compositions in both nonleached and strongly leached powders by using the site 1179 samples; comparisons between the leached and nonleached sample pairs are shown by yellow fields in supporting information Data Set S1. The results showed a systematic increase of 0.9–2.8 epsilon units in the Nd isotope composition after leaching. This change correlates with 9–15 epsilon unit decrease in Sr isotope composition (figure not shown; supporting information Data Set S1).

In contrast, the Hf isotope composition usually differed by only <0.7 epsilon units but one sample showed a 1.5 epsilon unit shift (supporting information Data Set S1). The results are consistent with those of our previous examination of the Japan seafloor basalts, which showed the same shift in the Nd isotope and an insignificant shift in the Hf isotope [Hirahara et al., 2015].

Additionally, the same test for Pb isotopes showed systematic shifts to radiogenic Pb perhaps through the seawater alteration; the tie lines for Site 1179 samples and the range are shown in Figure 4. These results are also consistent with the previous observations [Hauff et al., 2003].

We systematically tested the effect of leaching for only five Site 1179 MORB samples for four isotopes. The other MORB samples (Sites 1149, 801, 197, 303, and 304) analyzed in this study and the Hotta and Erimo-Bosei seamount samples were not leached. In contrast, the petit-spot basalts and the Shimanto greenstone samples were leached in order to remove the effect of alteration, which may be related to interaction with the seafloor sediment [Hirano et al., 2006; Machida et al., 2009] or accretionary prism sediments [Asaki and Yoshida, 1998; Kiminami et al., 1994] (supporting information Data Set S1). The age corrections for these leached and unleached samples were performed according to the element concentrations measured for the unleached and leached powders, respectively, following the method described in a previous study [Hanyu et al., 2011].

4.2. Trace Elements

Figure 5 plots all of the trace element data analyzed for the nonleached powder samples. In section 4.2.1, we describe the effects of alteration and geochemical features of the basalts analyzed in this study.

4.2.1. MORB Samples

Trace elements were newly analyzed for the MORBs from Sites 197, 303, 304, 1149, and 1179 and for the Shimanto and Yakushima greenstones. All of the DSDP/ODP MORBs are N-MORB type with positive spikes for K, U, Ba, Rb, and Cs, except for Site 304 MORBs, which showed no positive spikes for Rb and Cs (Figure 5). These enrichments are the result of seafloor alteration [Kelley *et al.*, 2003]. The greenstones from Shimanto and Yakushima are also N-MORB type with prominent element elevations in Sr, Pb, and U, together with enrichment in K, Ba, Rb, and Cs. The elevated levels of Sr and Pb are considered to be derived from assimilation with the host mudrocks, while the basalt magmas were hot [Asaki and Yoshida, 1998; Kiminami *et al.*, 1992] (Figure 5). However, the extent of enrichment differed slightly from those of other AOCs from the Pacific Plate except for Sr. Other than these alteration effects, the new results confirm the accreted N-MORB origin [Kiminami *et al.*, 1994] of the greenstones.

4.2.2. OIB and Petit-Spot Samples

All the basalts from the Hotta [Shimoda *et al.*, 2011] and newly analyzed Erimo and Bosei seamounts have compositions typical of OIBs [Sun and McDonough, 1989]. The analyzed petit-spot basalts are all OIB-type with enrichments in Sr, Pb, and Ba and strong depletions in heavy rare earth elements (Figure 5). The compositions are similar to those reported previously [Hirano *et al.*, 2006]. Moreover, they exhibit features similar to the EM1 basalts in NE China, which have been interpreted as the effects of an ancient sediment component in the source mantle [Kuritani *et al.*, 2011, 2013].

4.3. Pb Isotopes

The new Pb isotope data are shown in Figure 4 together with the previous data by the (t) correction treatment, as noted in section 4.1.

4.3.1. MORB Samples

The newly examined Pacific MORB samples from Sites 197, 304, 1149, and 1179 all plotted in the Pacific mantle field for Pb isotopes; these MORBs have the same isotopic composition as other Pacific MORBs from Sites 462, 800, 801, and 802A considering the effect of leaching (Figure 4). These results are essentially the same as those determined in previous work using MORBs from Sites 166, 197, 303, 304, 307, and 801 [Janney and Castillo, 1997]. The Shimanto and Yakushima greenstones are all N-MORB-type basalts that may have assimilated some of the ambient mudrocks (Figure 5). These leached greenstone basalts all fall in the Indian mantle field (Figure 4). This discrimination of provenance is reliable because any alteration effects should have shifted the Pb isotope composition to a more radiogenic direction. The Pb isotope ratios of the basalts could have still been affected by the sedimentary rocks, resulting in an increase of the EM2 sediment component [Plank and Langmuir, 1998]. In fact, the Shimanto and Yakushima greenstones plotted together on a straight mixing line, pointing to EM2; however, the other end of this mixing array pointed to the Indian mantle field, which is remarkably different from other Pacific MORBs (Figure 4).

4.3.2. OIB and Petit-Spot Samples

The Hotta Seamount OIBs plotted on the HIMU basalt field [Shimoda *et al.*, 2011], whereas the Erimo and Bosei OIBs were close to the FOZO of the Cook-Austral-type field [Stracke *et al.*, 2005] (Figure 4). The petit-spot basalts are isotopically distinctive from the OIBs, plotting in the EM1 field [Machida *et al.*, 2009] and overlapping the Indian mantle field [Mahoney *et al.*, 1998] with more radiogenic $^{208}\text{Pb}/^{204}\text{Pb}$ than that in the Shimanto MORBs (Figure 4). Even if the unleached results of the OIBs affected by the radiogenic Pb from alteration, the extent would not have altered the above conclusions. In contrast, the petit-spot basalts were strongly leached [Machida *et al.*, 2009] and were thus the results are unaffected by alteration (Figure 4). A linear trend between EM1 and EM2 composition is shown by the petit-spot basalts, which suggests some effects of assimilation of the Pacific seafloor sediment during intrusion [Machida *et al.*, 2009]; the same effect was detected in the Shimanto greenstones.

4.4. Nd-Hf Isotopes

As shown in section 4.1, Nd and Hf are less affected by post-eruption alterations and thus are ideal for tracing pristine mantle compositions recorded in the basalts of the Cretaceous to the Paleogene [Pearce *et al.*, 2007]. The Nd and Hf isotope data are displayed in Figure 6 as $\epsilon\text{Nd}(t)$ and $\epsilon\text{Hf}(t)$ using available age data and P/D element ratios. Similar to the Pb isotopes, P/D values are not always available for the Cretaceous seamount basalts; thus, we assumed OIB and MORB P/D values [Sun and McDonough, 1989] for these alkalic and tholeiitic basalts, respectively. The GEOROC [GEOROC, 2013] and PetDB databases [Class and Lehnert, 2012] were used for the ocean floor MORBs/OIBs (Figure 6a). Continental alkali basalt data from China and

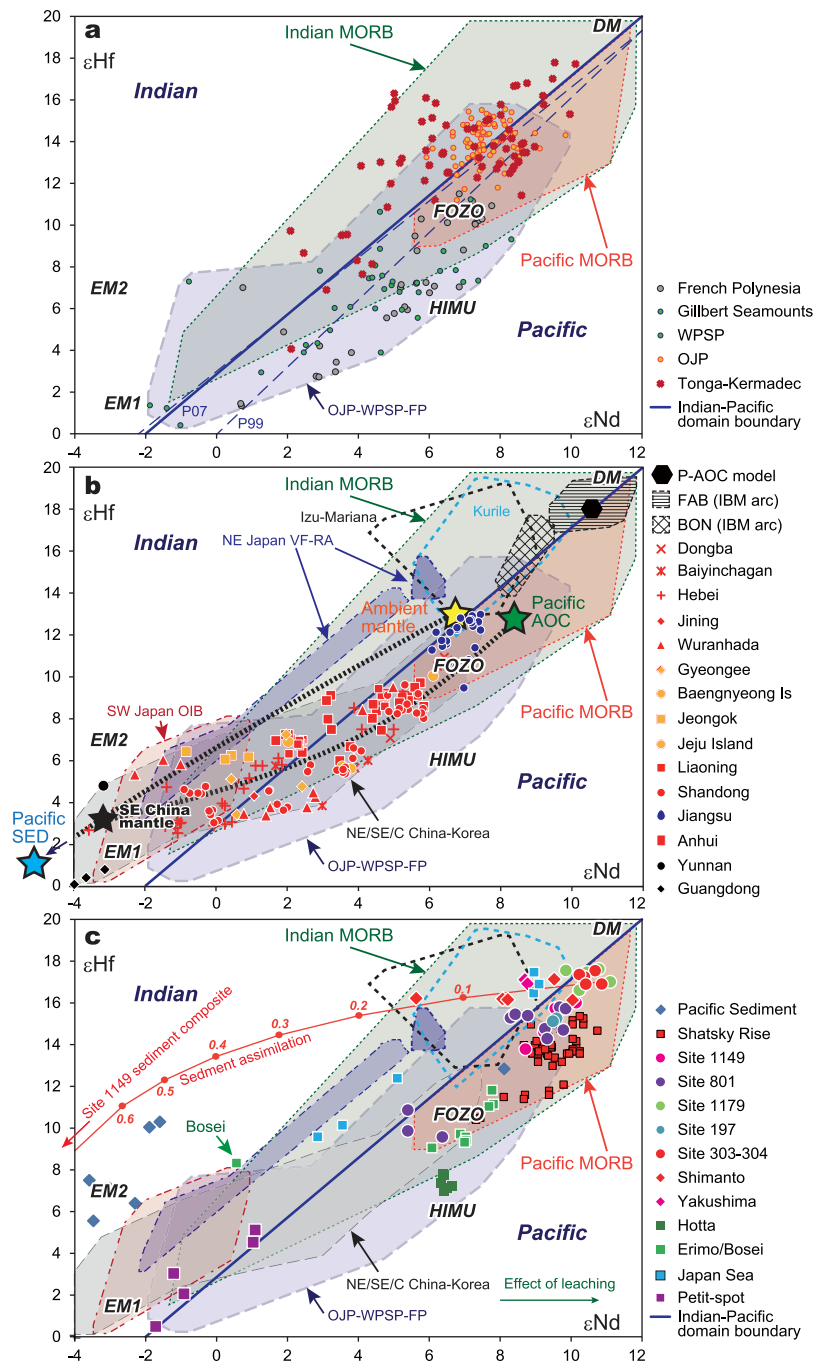


Figure 6. (a) ϵNd - ϵHf plots of the mid-ocean ridge basalts (MORBs) and ocean island basalts (OIBs) in the Pacific Ocean. (b) ϵNd - ϵHf compositions of the Cenozoic Izu-Mariana, SW Japan, NE Japan, and Kurile arc lavas with Cenozoic Eurasian continental basalts from Korea and China. All data are from the literature [Class and Lehnert, 2012; GEOROC, 2013]. (c) ϵNd - ϵHf data analyzed in this study were plotted with the Shatsky Rise basalts from the literature [Heydolph et al., 2014]. SE China mantle (black star), Pacific sediment (SED) (blue star), ambient mantle (yellow star), Pacific altered oceanic crust (AOC) (green star), and thick dotted mixing lines in Figure 6b are from Sakuyama et al. [2013]. Mixing line in Figure 6c is calculated from a Pacific MORB (Site 303 MORB from this study) and the average of the Site 1149 sediment composite [Chauvel et al., 2009]. The ϵHf and ϵNd values were calculated by using $^{176}\text{Hf}/^{177}\text{Hf}_{\text{CHUR}} = 0.282772$ after Blichert-Toft and Albarède [1997] and $^{143}\text{Nd}/^{144}\text{Nd}_{\text{CHUR}} = 0.512638$. The fields of Pacific and Indian MORBs, including Pacific and Indian mantle, are from supporting information Figure S1.

Korea were obtained from the literature [GEOROC, 2013; Sakuyama et al., 2013] (Figure 6b). Arc basalt data were obtained from Tonga-Kermadec [Pearce et al., 2007], Izu-Mariana [Pearce et al., 1999; Tollstrup et al., 2010; Woodhead et al., 2012], SW Japan [Kimura et al., 2010], NE Japan [Kimura and Nakajima, 2014; Kuritani

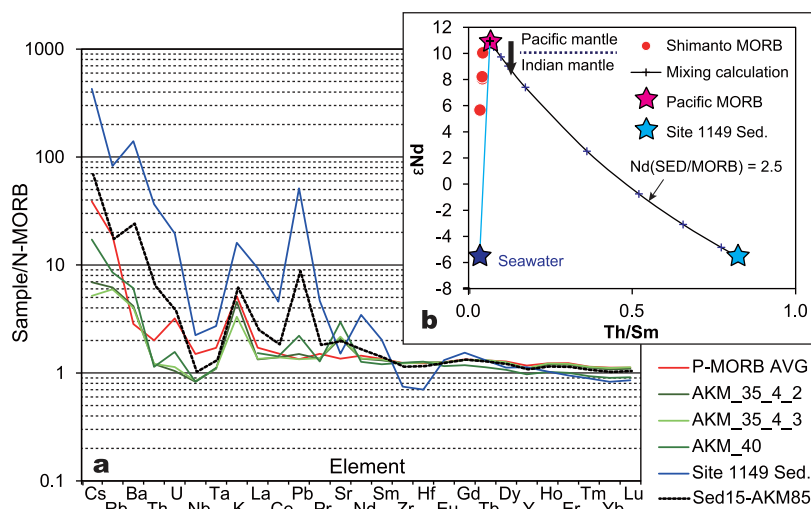


Figure 7. (a) Element abundances of the average Pacific Plate mid-ocean ridge basalts (P-MORB), accreted Shimanto MORBs, and averaged Pacific sediment represented by the Site 1149 sediment composite and (b) ϵ Nd-Th/Sm plots of the same samples. Mixing lines are from the observed Nd compositions in the P-MORB average and Site 1149 sediment, as shown by $\text{Nd}(\text{SED}/\text{MORB}) = 2.5$ and the seawater mixing line. Th, Nd, Sm, and Nd isotope compositions used for sediment calculations are from observed values. Those for seawater are from *Ama-kawa et al.* [2000]; *Chen et al.* [1986]; and *Zhang and Nozaki* [1996]. The Nd and Sm bulk P-MORB-sediment mixture does not support the observed ϵ Nd variation in the Shimanto MORBs. The Pacific and Indian mantle boundary is located at $\epsilon\text{Hf} = 18$. The thick vertical arrow shows the effect of maximum seawater alteration in $\epsilon\text{Nd} < -2.8$ by the leaching test. However, the ϵ Nd values of the Shimanto greenstones are from strongly leached samples; therefore, the effect has been eliminated. The Sed15-AKM85 line in Figure 7a shows a simple bulk mixing calculation between AKM_35_4_3 and Site 1149 sediment with elevated Th. The unleached Shimanto samples in Figure 7a do not show elevated Th, precluding assimilation of the host sediment.

et al., 2014; M. Ban *et al.*, JTABS project, unpublished data, 2015], Kurile [*Martynov et al.*, 2012], and Japan Sea floor basalts [*Hirahara et al.*, 2015] (Figure 6b). Additionally, DSDP/ODP sediment core sample data from southern Tonga [*Pearce et al.*, 2007] and Izu [*Chauvel et al.*, 2009] and basalt data from the Shatsky Rise [*Heydolph et al.*, 2014] are plotted in Figure 6c.

4.4.1. Nd-Hf Isotope Systematics

Nd-Hf isotope systematics is a useful tool for distinguishing mantle domains [*Nebel et al.*, 2007; *Pearce et al.*, 1999, 2007]. We re-examined the Pacific and Indian MORB fields based on the newly compiled database for the Pacific-Indian-Atlantic MORBs [*Class and Lehnert*, 2012]. The Indian-Pacific boundary passes through coordinates (ϵNd , ϵHf) = (-2, 0) and (12, 20) on the plot, as shown in Figure 6 and supporting information Figure S1; broken lines P99 and P07 in *Pearce et al.* [1999, 2007] can be used for comparison.

It is notable that the domain boundary can be defined only by the data distribution of the Pacific MORBs alone. The physiographic Indian MORB field overlaps the Pacific field, indicating involvement of the Pacific mantle component in the Indian mantle. Similar observations were revealed for the Atlantic MORB field, which suggests that the origin of the Atlantic mantle is the same as that of the Indian mantle. This feature indicates that Indian mantle is clearly identified when a basalt plots outside the Pacific mantle field and, most reliably, above the Indian-Pacific mantle boundary (Figure 6 and supporting information Figure S1). This feature differs completely from that shown by the $^{208}\text{Pb}/^{204}\text{Pb}$ - $^{206}\text{Pb}/^{204}\text{Pb}$ isotope systematics [*Mahoney et al.*, 1998] (Figure 4a).

4.4.2. MORB Samples

The Nd-Hf ratios were newly analyzed for the MORBs from Sites 197, 303, 304, 1149, and 1179. Including previously published data from Site 801 MORBs [*Chauvel et al.*, 2009] and the Shatsky Rise basalts [*Heydolph et al.*, 2014], the western Pacific MORB data plotted in the Pacific mantle field (Figure 6c). Our new data all fell in the Pacific mantle field except for one from Site 1179 and two from 801 that plotted slightly to the left of the mantle domain boundary. All the samples were unleached; thus, Nd isotopic compositions of the altered samples might shift by 1–1.5 epsilon units toward a more radiogenic composition (Figure 6c and supporting information Data Set S1).

The Shimanto and Yakushima greenstones show elevated ϵHf with various ϵNd forming a quasi-flat array in the Indian mantle field, with the most radiogenic Nd sample plotting in the Pacific mantle field (Figure 6c).

These greenstones were all strongly leached for isotope analysis in order to eliminate the effects of alteration (supporting information Data Set S1). Therefore, the flat array was, at first glance, thought to have formed through assimilation of the ambient mudrocks, as shown by field occurrences [Asaki and Yoshida, 1998; Kiminami *et al.*, 1994] and by the Pb isotopes (Figure 4). The calculated mixing hyperbola between a radiogenic Pacific MORB, represented by a Site 303 MORB, and an averaged Pacific sediment, represented by the Site 1149 sediment composite with $\epsilon_{\text{Nd}} = 4.4$ and $\epsilon_{\text{Hf}} = -5.9$, Nd = 25.2 ppm, and Hf = 1.44 ppm [Chauvel *et al.*, 2009], follow the observed data array. Assimilation of a 0.01–0.14 weight fraction of the sediment might explain the Shimanto MORB variation, as shown in Figure 6c.

Our close examinations, however, resulted in an opposite conclusion. A large amount of sediment addition should have altered the trace element compositions, such as increase in fluid immobile Th; However, this effect was not seen in the Shimanto greenstones, even when compared with the Pacific Plate MORBs (Figure 7a). A simple mixing of 15% Site 1149 sediment with 85% AKM35_4_3) increased the Th dramatically, although such an increase was not shown by the unleached Shimanto MORBs (Sed.15-AKM75 line in Figure 7a); the mixing rate from the maximum value was deduced from the mixing hyperbola in Figure 6c. Some back-arc basin basalts and almost all arc basalts have unradiogenic Nd and Hf [Hirahara *et al.*, 2015; Savov *et al.*, 2006] (see also Figure 6c). However, these basalts are always Th-enriched owing to the addition of the sediment component from the subducted slab [Hirahara *et al.*, 2015; Kimura and Nakajima, 2014; Plank, 2005]. However, this is not the case for the Shimanto greenstones, which exhibit even lesser amount of Th compared to the altered Pacific MORBs (Figure 7). Moreover, the Shimanto MORB with the most radiogenic Nd plotted in the Pacific mantle field (Figure 6b), which contradicts the results from the Pb isotopes showing the Indian mantle origin, at least in their nonradiogenic end composition (Figure 4).

To confirm these findings, we performed mixing calculations by using Th/Sm ratios sensitive to the sediment component assimilation [Plank, 2005] and ϵ_{Nd} and Nd compositions by using the Pacific MORB (Site 303) and Site 1149 sediment composite [Chauvel *et al.*, 2009; Plank *et al.*, 2007] (Figure 7b). The mixing between the sediment and Pacific MORB did not reproduce the observed ϵ_{Nd} variations, as shown by the mixing line using Nd(SD/MORB) = 2.5 (Figure 7b). The mixing calculations using a seawater composition [Amakawa *et al.*, 2000; Chen *et al.*, 1986; Zhang and Nozaki, 1996] showed a better fit, although such mixing requires tremendous amounts of seawater cycling (10^6 times MORB weight) between the host sediment and MORB. Some chemically precipitated sediments, such as chert, show no Th enrichment. However, the Shimanto sediments are almost all terrigenous in origin [Kiminami *et al.*, 1992, 1994].

The effect of seawater alteration did not decrease the value of ϵ_{Nd} greater than 1.6, as discussed in section 4.1 and in Hirahara *et al.* [2015]. The Shimanto MORB data are from strongly leached powders. We thus conclude that the ~70 Myr-old Shimanto MORBs and ~80 Myr-old Yakushima MORBs are from IPR-MORBs with Indian mantle provenance. This result is now consistent with the conclusion obtained from the Pb isotopes (Figure 4).

4.4.3. OIB and Petit-Spot Samples

In the $\epsilon_{\text{Nd}}-\epsilon_{\text{Hf}}$ plots, the Hotta and Erimo seamount OIBs plotted in the HIMU and FOZO fields [Stracke *et al.*, 2005], respectively (Figure 6c), which is consistent with those in the Pb isotopes (Figure 4). This indicates that the ~118 Myr-old seamounts currently near the Japan Trench are basically similar to the OIBs from the French Polynesian, Gilbert, and WPSP seamounts, all of which are considered to have originated from the SOPITA hotspot of deep mantle origin (Figures 1, 2, and 6) [Konter *et al.*, 2008; Koppers *et al.*, 2003; Shimoda *et al.*, 2011].

The petit-spot basalts have a clear EM1 characteristic in terms of Sr-Nd-Pb isotopes [Machida *et al.*, 2009]. The Nd-Hf isotope systematics also show an EM1 signature resembling both the nonradiogenic end composition of WPSP OIBs in plumes in the SOPITA area and of the Indian mantle as discussed for Pb isotopes (Figures 6c and 4 for Pb isotopes). The petit-spot basalts are also similar to the Eurasian EM1 basalts in the Nd-Hf systematics (Figure 6b).

The Hotta (HIMU), Erimo (FOZO) and Bosei (EM2) seamounts are located close to the petit-spot (EM1) volcano (Figure 1). The upper mantle beneath the Pacific Plate near the Japan Trench is thus locally heterogeneous. Small numbers of SOPITA OIBs have Nd-Hf isotopic signatures similar to those of the Bosei OIBs and petit-spot basalts. The EM1 and EM2 components are obviously present in plumes in the SOPITA area, although they are far less prominent than the other components (Figure 6a).

Overall, the EM signatures resembling the Indian mantle in the petit-spot basalts and Bosei OIBs likely originated from the deep mantle via the plumes in the SOPITA area. However, we note the possibility of the Indian mantle origin of the petit-spot basalts, as will be discussed in section 5.1.

4.4.4. Review of Basalts from Eastern Eurasian Margins

A widespread EM1 source mantle has been reported for the basalts in the eastern Eurasian plate margins from NE China and Korea [Choi *et al.*, 2006] and from SE China [Sakuyama *et al.*, 2013, 2014]. This was also shown by the Nd-Hf isotope systematics (Figure 6b).

The Nd-Hf isotope variation shown by all the basalts from SE, NE, and central China and Korea [GEOROC, 2013] (Figure 6) appears to have been formed by mixing between the EM1/EM2 source mantle (black star in Figure 6b), regardless of the formation process, with the HIMU-FOZO component [Choi *et al.*, 2006; Chu *et al.*, 2013] or with the ambient depleted Indian mantle and Pacific-type AOC (stagnant) slab component [Sakuyama *et al.*, 2013]. A few exceptions are shown by the Wudalianci volcano in NE China [Chu *et al.*, 2013] and the Ulleung and Dog Islands [Choi *et al.*, 2006], which have extreme values of EM1 with extremely nonradiogenic $\epsilon_{\text{Nd}} = -6$ to -1 and $\epsilon_{\text{Hf}} = -9$ to 0 out of the range of that shown in Figure 6, (not shown).

The variations of the continental Eurasian basalts overlap the Pacific OIBs with more weighted populations in the EM1 (and EM2). We note here that the weighted distribution of EM1 mantle is present beneath the continent. This result suggests a genetic link of EM1 to the subcontinental lithospheric mantle or the mantle asthenosphere above the mantle transition zone in the Eurasian deep subduction system.

5. Discussion

On the basis of the Pb-Nd-Hf isotope results and comparison with previous data, we discuss in this section the possible formation history of the missing western half of the Pacific Plate generated from the IPR, its relevance to the location of the Indian-Pacific mantle boundary, and its implications regarding the development of the mantle structure beneath the western Pacific. We first examine the nature and origin of the western Pacific mantle including marginal basins and Eurasia and propose that the location of the Indian-Pacific mantle boundary has been fairly stationary since ~ 80 Ma.

5.1. Nature of Indian Mantle Signatures

The sources for the IPR MORBs would have changed from the Pacific to the Indian mantle between ~ 130 and ~ 90 Ma [Straub *et al.*, 2010, 2015]. This is supported by the fact that the NW Pacific surface MORBs with ages of 160–130 Ma all plotted in the Pacific mantle field in both Pb and Nd-Hf isotope systematics (Figures 4 and 6), and that the Shimanto and Yakushima greenstone MORBs of ~ 80 –70 Ma are all of Indian mantle origin (Figures 4, 6, and 7). To ensure the interpretation of the geochemical data, we first need to answer to the first question raised in the Introduction: What is the source of the Indian mantle signature?

5.1.1. Which Isotope Should Be Used?

The Pb isotope composition of the mantle wedge is strongly affected by the subducted sediment and AOC fluxes in the supra-subduction environment, which is inherited by the compositions of the primary arc magmas [Kimura and Nakajima, 2014; Kimura *et al.*, 2010, 2014; Pearce, 2008; Straub *et al.*, 2009, 2015]. Thus, the Pb isotope compositions of arc magmas are usually inappropriate for estimating the wedge mantle composition unless the mantle composition is initially assumed by the composition of the back arc basin basalts, which are less affected by subduction, and the mass balance between the mantle and slab fluxes is carefully examined [Hickey-Vargas *et al.*, 1995; Kimura and Nakajima, 2014; Kimura *et al.*, 2014; Pearce, 2008; Straub *et al.*, 2015]. For example, the identification of the Indian-type Pacific Plate slab, proposed by Straub *et al.* [2015], is entirely dependent on the plots of Pb isotope ratios against Nd/Pb and Pb-Pb isotope plots. These diagrams essentially do not separate the contributions of radiogenic Pb from the slab sediment and AOC in the Marianas, as shown in Straub *et al.* [2015, Figures 15 and 16].

In contrast to Pb isotopes, the Nd-Hf isotope compositions are less affected by the slab fluxes unless the slab is either melted and the melt metasomatizes the mantle wedge in a hot subduction environment [Kimura *et al.*, 2014; Straub *et al.*, 2010; Tollstrup *et al.*, 2010], or solid slab material (i.e., slab sediment) is immediately introduced into the wedge mantle by its buoyancy [Behn *et al.*, 2011]. The latter could occur in a particular tectonic environment such as a back arc basin opening [Hirahara *et al.*, 2015]. Thus, we examined the Nd-Hf isotope systematics in the marginal basins and arcs in the western Pacific. For this analysis,

the Indian-Pacific mantle boundary was reasonably distinguished by the newly compiled Nd-Hf isotope data set from the Pacific and Indian-Atlantic ridges (Figure 6 and supporting information Figure S1). We thus used the same systematics for MORB, plume-sourced, supra-subduction, and continental lavas.

5.1.2. Plume Influenced Mantle Heterogeneity

The Pacific upper mantle is believed to have been modified by a large-scale SOPITA hotspot that has been active in the Pacific Ocean since the Cretaceous. The SOPITA-formed hotspot track is greater than 10,000 km long across the northwestern to southeastern Pacific and includes the WPSP [Koppers *et al.*, 2003] (Figures 1 and 2). The hotspot-related OIB decreases in age monotonically from the NW margins of the Pacific Plate (Bosei, Erimo, Hotta) at ~120 Ma [Shimoda *et al.*, 2011], through the WPSP seamounts of 100–70 Ma and Gilbert Seamounts of 70–43 Ma, to French Polynesia at 0 Ma [Koppers *et al.*, 2003], irrespective of the basement plate age. This relationship is consistent with the latest reconstruction of the plate since 140 Ma [Müller *et al.*, 2008] (Figure 2). The large plume head affected the upper mantle; thus, part of the Pacific upper mantle should exhibit enriched Indian mantle signatures represented by the involvement of EM1 (and even HIMU) components [Koppers *et al.*, 2003] (Figure 2). The EM1 and some EM2 mantle components in the OIBs in particular show radiogenic ^{207}Pb and ^{208}Pb at a given ^{206}Pb and radiogenic Hf at a given $^{143}\text{Nd}/^{144}\text{Nd}$; that is, they are isotopically indistinguishable from Indian mantle [Machida *et al.*, 2009; Stracke *et al.*, 2003].

Far smaller local-scale mantle heterogeneity is also present, as detected in the small-scale late Cenozoic (~6 Ma) alkali (petit-spot) volcanoes that erupted EM1 basalts on the ~140 Myr-old western Pacific Plate [Hirano *et al.*, 2006] (Figure 1). The petit-spot mantle could have formed by a locally modified mantle by the SOPITA hotspot in the past or through rigorous mantle convection that dispersed recycled materials, as previously interpreted [Machida *et al.*, 2009]. Alternatively, the petit-spot basalts represent typical EM1 Indian mantle without the influence of a plume [Hofmann and Hart, 2007], as discussed in section 4) If so, the petit-spot basalts represent the presence of the Indian mantle beneath the Pacific Plate at ~6 Ma about 1100 km from the Kurile-Japan-Nankai-Ryukyu Trench at that time. This theory is supported by the increase in EM1 component in the upper mantle toward the Eurasia continent (Figure 6b).

Although local Indian mantle-like enriched EM1 mantle are contaminated in the Pacific mantle, the following issues remain to be addressed under this scenario: (1) the manner in which the huge Pacific Plate slab generated from the IPR could change its composition from Depleted Pacific MORB-type to Depleted Indian MORB-type ocean crust sometime between 130 Ma and ~80 Ma, and (2) the relationship of this event to the present-day Indian-Pacific mantle boundary. We address these issues in section 5.2.

5.1.3. Supra-Subduction Zone Mantle Heterogeneity

Before addressing the aforementioned issues, we need to re-evaluate the mantle beneath the western Pacific marginal basins where the Indian MORB mantle is believed to occupy the upper mantle. This discussion immediately relates to the first argument raised by the proposal by Straub *et al.* [2009], such that the Indian mantle “flavor” in the arc lavas is partly from the altered oceanic crust rather than entirely from the wedge mantle. By examining the effects of subducted sediment and AOC, we can examine the mantle source in the marginal basins.

The Nd-Hf isotope compositions of the basalts in the Tonga-Kermadec arc, including the Havre Trough back arc basin basalt, mostly plotted in the Indian mantle field (Figure 6a). This led Pearce *et al.* [2007] to conclude that the Indian mantle origin of the wedge mantle and the surface of the subducting Pacific Plate slab is the boundary of the Indian-Pacific mantle domains. The same model was also proposed for the Izu-Bonin-Mariana subduction systems and the Philippine Sea plate back arc basin using Nd-Hf isotope data [Pearce *et al.*, 1999; Woodhead *et al.*, 2012]. Straub *et al.* [2015] accepted this consensus and examined the Mariana arc-Mariana Trough system using Nd-Hf isotope systematics. They confirmed that the Mariana arc mantle has Indian mantle provenance, as shown in their Figure 12. The mantle wedge beneath the N-Izu arc also shows Indian mantle provenance, as shown in Tollstrup *et al.* [2010, Figure 7]. The back arc basin mantle beneath the entire Philippine Sea Plate, including the mantle wedge beneath the arcs, is entirely Indian mantle, as shown in the Izu-Mariana field in Figure 6b). Small EM1 blobs [Ishizuka *et al.*, 2009], and even HIMU mantle blobs [Li *et al.*, 2013], have been identified in the Izu-Mariana arc-back arc system, further suggesting the existence of an extreme Indian mantle in the mantle wedge.

The Japan Sea back arc basin and its relevant NE Japan subduction zone is another example in which Pb isotope data of the Japan back arc basin basalts show strong Indian mantle provenance with elevated ratios

of $^{207}\text{Pb}/^{204}\text{Pb}$ and $^{208}\text{Pb}/^{204}\text{Pb}$ [Flower *et al.*, 2001; Kimura and Nakajima, 2014; Kimura *et al.*, 2006; Okamura *et al.*, 2005]. Recently, Hf isotope data have become available for the basalts from SW Japan [Kimura *et al.*, 2014], NE Japan [Kimura and Nakajima, 2014; Kuritani *et al.*, 2014], and the Japan Sea back arc basin [Hirahara *et al.*, 2015] (Figure 6). The role of subcontinental mantle beneath Eurasia should also be considered because the mantle beneath the Japan Sea was previously thought to be subcontinental lithospheric mantle or depleted subcontinental asthenosphere [Okamura *et al.*, 2005]. In fact, strong EM1 components have been reported from the basalts in and around the Japan Sea [Nohda, 2009; Pouclet *et al.*, 1995]. The fragments of subcontinental lithospheric mantle would currently be present in the mantle lithosphere [Okamura *et al.*, 2005] or would be eroded from the subcontinental lithospheric mantle during the opening of the marginal basins or break-up of the continent; these fragments would have later upwelled with a mantle plume or through convection to generate basalts with EM1 and EM2 components [Hoernle *et al.*, 2011]. The mantle wedges of the associated Kurile-Japan-Nankai arcs are believed to be depleted Indian mantle but are potentially influenced by the subcontinental lithospheric mantle by any mechanism.

According to observation, all of the Japan seafloor basalts plotted well within the Indian mantle field in Nd-Hf isotope systematics, including the depleted type (D-type) basalts in the depleted Indian MORB field (Figure 6c). The wide and linear variations of the enriched type (E-type) basalts are considered to be the result of mixing of the bulk slab sediment with the depleted Indian mantle, melted together in an adiabatically upwelled mantle during the opening of the Japan Sea about 17–15 Ma [Hirahara *et al.*, 2015]. This indicates that the depleted Indian MORB-source mantle is widespread beneath the Japan Sea.

The relevant NE Japan arc volcanic front (VF) lavas are considered to form mixtures between the mantle and enriched crustal components [Kimura and Yoshida, 2006; Kimura and Nakajima, 2014], showing a linear array in the Indian mantle field in the Nd-Hf isotope plots (NE Japan VF-RA in Figure 6b). The radiogenic end of the mixing array should therefore indicate the mantle composition beneath NE Japan. In fact, the rear-arc (RA) basalts from Chokai or Sannomegata volcanoes (Figure 1b), which are less affected by crustal assimilation [Kimura and Yoshida, 2006; Kimura and Nakajima, 2014; Kuritani *et al.*, 2014], plotted within the Indian mantle field shown by the Izu-Marianas. These basalts are slightly less radiogenic than the D-type Japan Sea floor basalts, suggesting the presence of a common depleted Indian mantle in the NE Japan mantle wedge (Figure 6c).

Exceptions are the OIB-type basalts, such as Kannabe and part of Abu volcanoes (Figure 1b), which were unaffected by the subducting Philippine Sea Plate slab flux in the SW Japan arc. These basalts are believed to represent the mantle composition beneath SW Japan [Kimura *et al.*, 2014]. The Nd-Hf isotope compositions of the SW Japan arc OIBs overlap the EM1 and EM2 mantle in SE, NE, and central China and Korea (Figure 6b), indicating that the same EM1-EM2 sub continental mantle is present beneath the arc. This theory is consistent with the remnant continental fragment moving away during opening of the Japan Sea [Kimura *et al.*, 2005].

On the basis of the Nd-Hf isotope systematics of the basalts from the western Pacific arcs and marginal basins, we conclude that the western Pacific marginal basin mantle above the Pacific Plate slab is entirely depleted Indian mantle with occasional EM1-EM2 components. The depleted Japan Sea Indian mantle almost overlaps the Tonga-Kermadec-Havre Trough and Izu-Mariana-Philippine Sea Plate mantle fields, suggesting the same depleted Indian mantle origin (Figure 6c). Moreover, the basalts from the Kurile arc also overlap the depleted Indian MORB field, indicating the Indian mantle provenance of the mantle wedge [Martynov *et al.*, 2012] (Figure 6b). This strongly supports the previous consensus that the present-day surficial mantle domain boundary is located along the western Pacific Kurile-Japan-Izu-Mariana-Vitiaz-Tonga Trench (Figure 1) [Flower *et al.*, 2001; Machida *et al.*, 2009; Nebel *et al.*, 2007; Pearce *et al.*, 1999].

5.1.4. Subcontinental Mantle Heterogeneity

The presence of depleted Indian mantle, EM1, and some EM2 components in the Eurasian continental basalts results in a significant mantle heterogeneity beneath the continent. In Figure 6b, the most depleted continental basalt data in the Jiangsu region are plotted close to the depleted Indian MORB mantle field defined by the western Pacific marginal basins. The sources of the enriched mantle dominant in EM1 beneath Eurasia could be (1) the sub continental lithospheric mantle [Chu *et al.*, 2013; Hoernle *et al.*, 2011; Okamura *et al.*, 2005; Pouclet *et al.*, 1995], (2) delaminated lower crust [Carlson *et al.*, 1996; Hawkesworth *et al.*, 1986; Willbold and Stracke, 2006], (3) a mantle transition zone affected by ancient subduction [Kuritani *et al.*, 2011], (4) stagnant Pacific Plate AOC [Sakuyama *et al.*, 2013] and sediments [Hirahara *et al.*, 2015];

Sakuyama et al., 2014] relevant to the prolonged evolution of the subducted slab components in the mantle transition zone since the Archean to the present in the supercontinental root. *Sakuyama et al.* [2013] suggested that the continental basalt array was formed by mixing between the subcontinental EM1 asthenospheric mantle (black star in Figure 6b) and the deep subducted stagnant slab AOC component currently present at the mantle transition zone (green star); the EM1 component was formed by mixing between the depleted mantle (yellow star) and the sediment component (blue star) [*Sakuyama et al.*, 2013, 2014]. The composition of the depleted Indian mantle (Jiangsu: yellow star) is akin to the mantle beneath the western Pacific marginal basins and is distinct from the subduction and crustal components. Therefore, the depleted Indian mantle should be a common component of the mantle beneath the Eurasia regardless of the mixing model (Figure 6b).

The isotopic similarity in EM1 (Figures 4 and 6) and the commonly elevated Ba/La and K/La ratios in the OIB EM1 [*Willbold and Stracke*, 2006], petit-spot EM1 basalt [*Hirano et al.*, 2006] (Figure 5), and continental EM1 basalt [*Chu et al.*, 2013; *Kuritani et al.*, 2011, 2013] suggest a similar formation process of the EM1 mantle. EM1 could have been formed in the mantle transition zone by addition of the subducted sediment via a prolonged subduction activity [*Kuritani et al.*, 2011, 2013] or by delamination of the lower continental crust into the deep mantle [*Carlson et al.*, 1996; *Hawkesworth et al.*, 1986; *Willbold and Stracke*, 2006]. A discussion on the origin of the enriched mantle component is beyond the scope of this paper. However, the long-lived stationary mantle boundary (SMB) in the western Pacific proposed in the following subsection would be relevant to the argument of continental versus oceanic separation of the large mantle domains at least till the depth of the mantle transition zone.

5.2. SMB Model for Indian and Pacific Mantle

On the basis of the above discussions, we propose an SMB model for the upper mantle boundary between the Indian and Pacific mantles. The discussions in the preceding sections confirm the present-day Indian-Pacific mantle boundary based on (Pb-)Nd-Hf isotope systematics; this conclusion is essentially unchanged from the previous consensus [*Pearce et al.*, 2007; *Straub et al.*, 2010, 2015]. Furthermore, our examinations on the Shimanto greenstone MORBs provide the first direct evidence for the Indian mantle origin of the IPR MORB.

The remaining second question raised in the Introduction to be answered concerns the location of the Indian-Pacific mantle boundary prior to subduction of the IPR (60–55 Ma) and beneath the present-day Pacific Plate. The model should address the following points: (1) the change in the IPR MORBs from Pacific- to Indian-type that occurred sometime between ~130–80 Ma and (2) the retention of the Indian mantle above the Pacific Plate, at least after ~50 Ma, in the Izu-Mariana arc, the Philippine Sea Plate back arc basin system [*Pearce et al.*, 1999; *Straub et al.*, 2015], and the NE Japan arc-Japan Sea back arc basin system [*Okamura et al.*, 2005].

5.2.1. Location of Indian-Pacific SMB

Figure 8 shows an evolutionary model of the upper mantle and oceanic plate in the Pacific including Eurasian margin subduction zones. The upper mantle beneath the Pacific Ocean basin is largely occupied by the depleted Pacific mantle domain. In contrast, the upper mantle beneath the western Pacific marginal basins and the Eurasian continent is occupied by the depleted Indian mantle (Figures 8a–8c). The subducted oceanic crust beneath the Indian mantle is entirely of IPR origin, formed from the Pacific mantle in 180–130 Ma (Pacific ocean floor MORBs) and from the Indian mantle with a plate age of ~80 Ma (Yakushima) to ~70 Ma (Shimanto) (Figures 8b–8c). The passage of IPR over the Pacific-Indian mantle boundary should have occurred somewhere in the western Pacific basin between 130 Ma and 80 Ma, by the time of IPR subduction beneath the Eurasian continent at 60–55 Ma (Figure 8b).

If the estimates of Indian-type AOC subductions occurring at 42–15 Ma at N-Izu and at 24–10 Ma in the Marianas [*Straub et al.*, 2015] are correct, the formation ages of the subducted Indian-type Pacific Plate are about 100 Ma and 90 Ma, respectively. Both parts of the Pacific Plate belonged to the eastern wings of the IPR at that times, as shown in *Sdalias and Müller* [2006, Figure 4b]. Therefore, the *Straub et al.* [2015] model requires location of the stationary Indian-Pacific mantle boundary far east to midway of the present Pacific Ocean basin (thin dotted lines in Figure 8 [*Straub et al.*, 2015, Figure 20, right]).

A problem with the far-east boundary model is the Detroit Seamount (~76–81 Ma) of the oldest Emperor Chain volcano in the Hawaiian hotspot track. The seamount was located on the ~100 Myr-old Pacific Plate

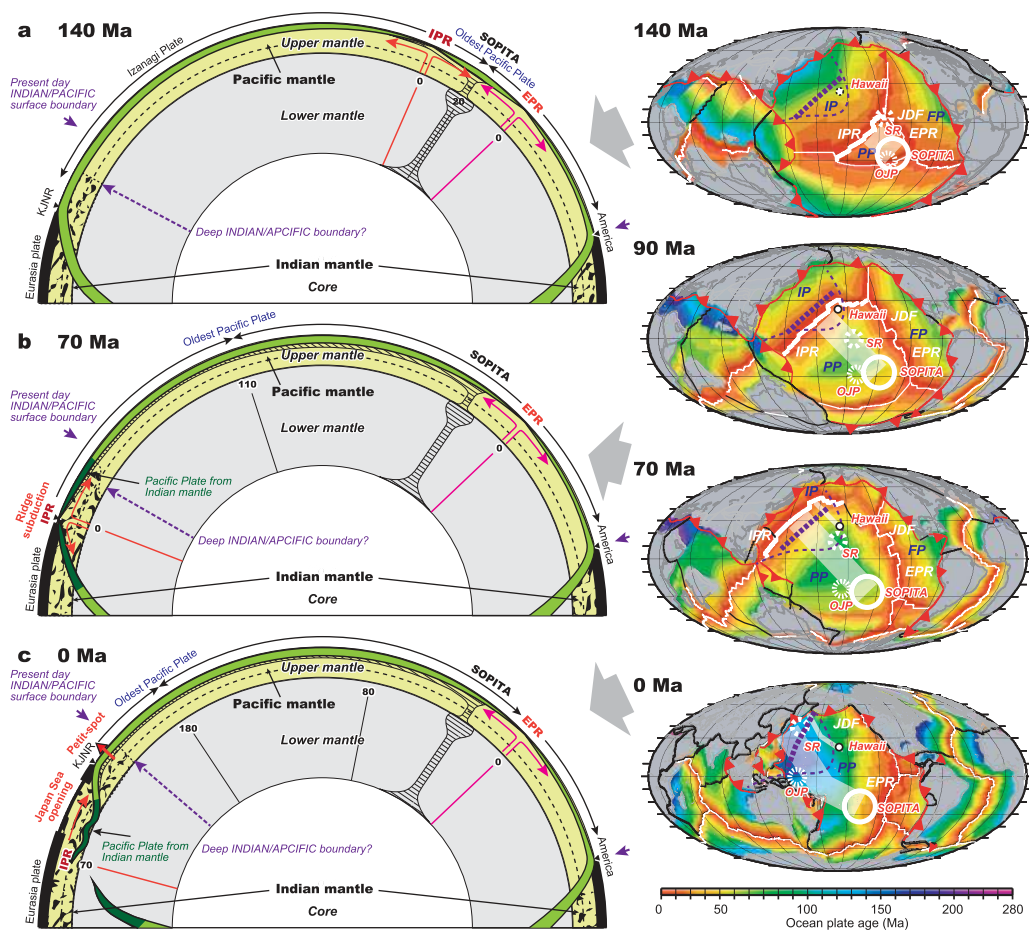


Figure 8. Schematic cross sections showing the growth of the Izanagi-Pacific Ridge (IPR) and its relationship to the Indian-Pacific mantle domain boundary. Paleogeographic maps on the right were adopted from literature [Müller *et al.*, 2008] and modified by the authors, as shown in Figure 2. IP: Izanagi Plate; FP: Farallon Plate; PP: Pacific Plate; JDF: Juan de Fuca Ridge; EPR: East Pacific Rise; SOPITA: South Pacific Thermal and Isotopic Anomaly; OJP: Ontong Java Plateau; SR: Shatsky Rise; Hawaii: Hawaii hotspot; KJNR: Kurile-Japan-Nankai-Ryukyu Trench. The thick deep-purple broken line represents the Indian-Pacific mantle domain boundary (this study). The thin deep-purple broken line represents Indian-Pacific mantle domain boundary proposed by Straub *et al.* [2015]. The transparent white lines indicate hotspot tracks of SOPITA and Hawaii. The small numbers in the left-hand plots indicate plates at given ages. Location of the sunken Izanagi Plate may be deeper according to the geodynamic model [Seton *et al.*, 2015].

near IPR, as shown in *Sdovias and Müller* [2006, Figure 5a]. The erupted tholeiite basalts have been dated as old as 81 Ma and show depleted Nd-Sr-Pb isotopic compositions very similar to EPR MORBs. However, more enriched basalts somewhat similar to the rejuvenated stage Hawaiian hotspot basalts in terms of Ba/Th and Sr isotopic compositions are also associated, although these lavas show Pb isotopic signatures of Pacific mantle origin [Huang *et al.*, 2005]. These features are interpreted as Hawaiian plume-IPR ridge interactions and the ambient near-IPR mantle is supposed to be Pacific-type by 81 Ma [Huang *et al.*, 2005]. This contradicts the passage of IPR over the Indian-Pacific mantle boundary at 100–90 Ma proposed by *Straub et al.* [2015] (Figure 8; thin dotted line in 90 Ma right plot), in which the Indian mantle underlay the Detroit Seamount well before 90 Ma. We conclude that the passage of IPR over the Pacific-Indian mantle boundary occurred at ~80 Ma because the IPR should be younger than the oldest known MORB-type tholeiite (81 Ma) in the Detroit Seamount.

The paleogeography of the Philippine Sea Plate is enigmatic because the edges of the plate are surrounded entirely by subduction zones [Hall, 2002]. This may affect relative locations between the N-Izu and Mariana arcs and the Pacific Plate. We thus leave this question open for the Equatorial western Pacific and await the results of future works. However, the concept that the Indian-Pacific mantle domain boundary existed beneath the Pacific Plate prior to the initiation of subduction [Pearce and Parkinson, 1993; Straub *et al.*, 2015] is consistent with our SMB model, which indicates that the IPR crossed this preexisting Indian-Pacific

mantle boundary in the western Pacific Ocean basin at ~ 80 Ma, prior to the initiation of subduction of the Izu-Bonin-Mariana arc at ~ 52 Ma.

5.2.2. Indian-Pacific SMB in the Past 140 Myr

The reconstruction of plate motion [Müller *et al.*, 2008; Sdolias and Müller, 2006] and the source change of the IPR mantle at ~ 80 Ma (this study) (Figure 8) suggest that the position of the Indian-Pacific upper mantle boundary has been stationary, whereas the Pacific Plate slab moved almost freely over the Indian-Pacific mantle boundary. The IPR spreading ridge crossed the boundary around ~ 80 Ma (Figures 8a–8c). The passage of the IPR might have caused spreading of the uppermost Indian mantle E-W (Figure 8b). Therefore, the Indian-Pacific mantle boundary could have been extended slightly to the east by the drag force (Figure 8b).

Subsequent rigorous opening of the Japan Sea from ~ 35 Ma to 15 Ma [Okamura *et al.*, 2005] caused by slab rollback [Sdolias and Müller, 2006] would have brought the Indian mantle beneath the Eurasian continent horizontally eastward, forming widespread depleted Indian mantle beneath the marginal basins (Figure 8c). This hypothesis is supported by the Pb isotopes reported by Flower *et al.* [2001] and by our Nd-Hf isotope systematics. Accreted Shimanto greenstone MORBs (~ 80 –70 Ma) offer direct evidence of the depleted Indian mantle existing in the western Pacific prior to IPR subduction. If the petit-spot EM1 basalts were the enriched part of the Indian mantle in origin rather than leftover EM1 by the plumes in the SOPITA area, the present Indian-Pacific mantle boundary more than 1100 km off from the Japan Trench at ~ 6 Ma, which is the approximate distance to the Shatsky Rise (Figure 8c, 0 Ma, right). In combination with the plate reconstruction in the literature [Müller *et al.*, 2008], the geographic location of the Indian-Pacific mantle boundary has been fairly stationary, and the passage of the IPR over the mantle boundary around ~ 80 Ma was thought to be almost subparallel to the boundary (Figures 8a–8c, right).

The above conclusion is the most applicable for the Japan Trench and Japan Sea back arc basin system. Events occurring in the Izu-Bonin-Mariana arc-back arc basin system need further examination. The mantle wedge composition immediately after the initiation of Pacific Plate subduction at ~ 52 Ma is regarded as Indian mantle, based on the Nd-Hf isotope compositions from the infant fore arc basalts, boninites at ~ 48 Ma, and Eocene arc tholeiite basalts [Reagan *et al.*, 2010] (Figure 6b). The composition of the incoming Pacific Plate AOC is either Indian or Pacific mantle, based on the mass balance modeling of boninite formation [Li *et al.*, 2013] (Figure 6b). Therefore, poor constraint is still given to this factor.

Additionally, the enriched-depleted variation in the Indian mantle is stronger than that in the Pacific mantle, reflecting the contribution of recycled EM1 and EM2 components (Figure 6). The depleted Indian mantle is dominant in the marginal basins (Figures 6a and 6b) and in the mantle beneath the western Pacific (Figure 6c). Progressive continent-ward enrichment in EM1 and EM2 components is obvious, which relates to the prolonged subduction components [Kuritani *et al.*, 2011; Rehkamper and Hofmann, 1997]. However, the origin of the depleted Indian mantle itself should also be explored along with the depleted Pacific mantle for comprehensive understanding of the hemispheric-scale mantle heterogeneity. This, along with the origin of the enriched mantles, is beyond the scope of the present paper; however, our results shed light on problems incurred in the analysis of spatial distribution of mantle sources.

6. Conclusions

We examined the Pb-Nd-Hf isotope and trace element compositions of MORBs from borehole cores obtained in the western Pacific, accreted MORBs to the Cretaceous-Paleogene accretionary prism along the northwestern Pacific subduction zones, OIBs from Cretaceous seamounts, and basalts from petit-spot volcanoes in the northwestern Pacific. The results show that all of the surficial Pacific Plate MORBs of 160–130 Myr old have Pacific mantle provenance, whereas the accreted MORBs of ~ 80 –70 Myr old from the subducted IPR have Indian mantle origins. The OIBs and petit-spot basalts are from variously enriched sources of EM1, EM2, HIMU, and FOZO. The upper mantle beneath the Pacific Ocean basin is entirely Pacific mantle, forming a large Pacific mantle domain; however, it is influenced by the hotspot track of the SOPITA. In contrast, the mantle that formed the IPR MORB between ~ 80 Ma and 70 Ma was Indian mantle. The western Pacific marginal basins are also Indian mantle, irrespective of the mantle wedge beneath the subduction zones, back arc basins, and Eurasian subcontinental mantle. We interpret that the IPR spreading ridge passed over the Indian-Pacific mantle boundary at ~ 80 Ma and subducted beneath the Eurasian Plate at

65–55 Ma. The Indian-type MORBs have therefore been subducted beneath the Eurasia continent and are now stagnated in the mantle transition zone. Therefore, the location of the Indian-Pacific mantle boundary has remained almost stationary in the western Pacific, irrespective of the surface plate boundary (e.g., IPR). The results of our SMB model for the upper mantle indicate that the Indian mantle has radiogenic Pb and Hf, suggesting significant inputs of subducted EM1 and EM2 components over the geologic past. Subduction-influenced subcontinental mantle of the Eurasian continent (Gondwana supercontinent) versus the Pacific mantle unaffected by subduction would have been unmixed at least in the upper mantle, although plume-influenced enriched materials do exist beneath the Pacific.

Acknowledgments

We are grateful for the valuable discussions with James B. Gill and Robert J. Stern. Data for Sites 197, 303, and 404 DSDP and ODP legacy core samples were provided by the International Ocean Drilling Program core repository at Texas A&M University. Constructive review comments from Jasper Konter, Jo Whittaker, and an anonymous reviewer improved the manuscript considerably. We are also thankful for editorial handling by the journal editor Janne Blichert-Toft. This work was partly supported by the Japan Society for the Promotion of Science (JSPS) research grants 24340136 and 15H02148 to JJK. Maps used in Figure 1 were generated by Generic Mapping Tool (GMT version 6.1) [Wessel and Smith, 1998] with digital elevation data of GTOPO30 from the USGS [United State Geological Survey, 2000] and of ETOPOS from NOAA [National Oceanic and Atmospheric Administration, 2000]. Paleogeographic maps used in Figure 2 are from the literature [Müller et al., 2008]. Figure 3 is drawn from Sakuyama et al. [2013, Figure 1]. Data used in Figure 4 are from references noted in the text and from our new data given in the supporting information Data Set S1. Data used in Figure 5 are given in the supporting information Data Set S1. Data used in Figures 6 and 7 are from references noted in the text and from our own data given in the supporting information Data Set S1. Paleogeographic maps used in Figure 8 are from the literature [Müller et al., 2008]. Data used in supporting information Figure S1 are from the references in the supporting information PDF.

References

- Allegre, C. J., and D. L. Turcotte (1986), Implications of a two-component marble-cake mantle, *Nature*, **323**, 123–127.
- Amakawa, H., D. S. Alibo, and Y. Nozaki (2000), Nd isotopic composition and REE pattern in the surface waters of the eastern Indian Ocean and its adjacent seas, *Geochim. Cosmochim. Acta*, **64**, 1715–1727, doi:10.1016/S0016-7037(00)00333-1.
- Asaki, T., and T. Yoshida (1998), Subduction-zone type greenstones from the northern Shimanto belt in southern Tokushima Prefecture, Southwest Japan, *J. Mineral. Petrol. Econ. Geol.*, **93**, 83–102.
- Baker, J., D. Peate, T. Waight, and C. Meyzen (2004), Pb isotope analysis of standards and samples using ^{207}Pb – ^{204}Pb double spike and thallium to correct for mass bias with a double-focusing MC-ICP-MS, *Chem. Geol.*, **211**, 275–303, doi:10.1016/j.chemgeo.2004.06.030.
- Behn, M. D., P. B. Kelemen, G. Hirth, B. R. Hacker, and H.-J. Massonne (2011), Diapirs as the source of the sediment signature in arc lavas, *Nat. Geosci.*, **4**, 641–646, doi:10.1038/NGEO1214.
- Blichert-Toft, J., and F. Albarède (1997), The Lu–Hf isotope geochemistry of chondrites and the evolution of the mantle crust system, *Earth Planet. Sci. Lett.*, **148**, 343–258, doi:10.1016/S0012-821X(97)00040-X.
- Carlson, R. W., S. Esperança, and D. P. Svisero (1996), Chemical and Os isotopic study of Cretaceous potassic rocks from Southern Brazil, *Contrib. Mineral. Petrol.*, **125**(4), 393–405, doi:10.1007/s004100050230.
- Chang, Q., T. Shibata, K. Sinotsuka, M. Yoshikawa, and Y. Tatsumi (2003), Precise determination of trace elements in geological standard rocks using inductively coupled plasma mass spectrometry (ICP-MS), *Frontier Res. Earth Evol.*, **1**, 357–362.
- Chauvel, C., and J. Blichert-Toft (2001), A hafnium isotope and trace element perspective on melting of the depleted mantle, *Earth Planet. Sci. Lett.*, **190**, 137–151.
- Chauvel, C., J.-C. Marini, T. Plank, and J. N. Ludden (2009), Hf–Nd input flux in the Izu–Mariana subduction zone and recycling of subducted material in the mantle, *Geochim. Geophys. Geosyst.*, **10**, Q01001, doi:10.1029/2008GC002101.
- Chen, J. H., R. Lawrence Edwards, and G. J. Wasserburg (1986), ^{238}U , ^{234}U and ^{232}Th in seawater, *Earth Planet. Sci. Lett.*, **80**, 241–251, doi:10.1016/0012-821X(86)90108-1.
- Choi, S. H., S. B. Mukasa, S.-T. Kwon, and A. V. Andronikov (2006), Sr, Nd, Pb and Hf isotopic compositions of late Cenozoic alkali basalts in South Korea: Evidence for mixing between the two dominant asthenospheric mantle domains beneath East Asia, *Chem. Geol.*, **232**, 134–151, doi:10.1016/j.chemgeo.2006.02.014.
- Chu, Z.-Y., J. Harvey, C.-Z. Liu, J.-H. Guo, F.-Y. Wu, W. Tian, Y.-L. Zhang, and Y.-H. Yang (2013), Source of highly potassic basalts in northeast China: Evidence from Re–Os, Sr–Nd–Hf isotopes and PGE geochemistry, *Chem. Geol.*, **357**, 52–66, doi:10.1016/j.chemgeo.2013.08.007.
- Class, C., and K. Lehnert (2012), PetDB expert MORB (mid-ocean ridge basalt) compilation, *EarthChem Libr.*, doi:10.1594/IEDA/10060.
- Condie, K. C. (2001), *Mantle Plumes and Their Record in Earth History*, Cambridge Univ. Press, Cambridge, U. K.
- Davies, G. F. (2009), Reconciling the geophysical and geochemical mantles: Plume flows, heterogeneities, and disequilibrium, *Geochim. Geophys. Geosyst.*, **10**, Q10008, doi:10.1029/2009GC002634.
- Dupré, B., and C. J. Allègre (1983), Pb–Sr isotopic variation in Indian Ocean basalts and mixing phenomena, *Nature*, **303**, 142–144, doi:10.1038/303142a0.
- Farnetani, C. G., and A. W. Hofmann (2010), Dynamics and internal structure of the Hawaiian plume, *Earth Planet. Sci. Lett.*, **295**, 231–240, doi:10.1016/j.epsl.2010.04.005.
- Flower, M. F. J., R. M. Russo, K. Tamaki, and N. Hoang (2001), Mantle contamination and the Izu–Bonin–Mariana (IBM) ‘high-tide mark’: Evidence for mantle extrusion caused by Tethyan closure, *Tectonophysics*, **333**, 9–34, doi:10.1016/S0040-1951(00)00264-X.
- Fukao, Y., M. Obayashi, H. Inoue, and M. Nishii (1992), Subducting slabs stagnant in the mantle transition zone, *J. Geophys. Res.*, **97**, 4809–4822, doi:10.1029/91JB02749.
- GEOROC (2013), GEOROC: Geochemistry of Rocks of the Oceans and Continents. [Available at <http://georoc.mpch-mainz.gwdg.de/georoc/>]
- Hall, R. (2002), Cenozoic geological and plate tectonic evolution of SE Asia and the SW Pacific: Computer-based reconstructions, model and animations, *J. Asian Earth Sci.*, **20**, 353–431, doi:10.1016/S1367-9120(01)00069-4.
- Hanan, B. B., and D. W. Graham (1996), Lead and helium isotope evidence from oceanic basalts for a common deep source of mantle plumes, *Science*, **272**(5264), 991–995, doi:10.1126/science.272.5264.991.
- Hanan, B. B., J. Blichert-Toft, D. G. Pyle, and D. M. Christie (2004), Contrasting origins of the upper mantle revealed by hafnium and lead isotopes from the Southeast Indian Ridge, *Nature*, **432**(7013), 91–94, doi:10.1038/nature03026.
- Hanyu, T., Y. Tatsumi, R. Senda, T. Miyazaki, Q. Chang, Y. Hirahara, T. Takahashi, H. Kawabata, K. Suzuki, and J.-I. Kimura (2011), Geochemical characteristics and origin of the HIMU reservoir: A possible mantle plume source in the lower mantle, *Geochim. Geophys. Geosyst.*, **12**, Q0AC09, doi:10.1029/2010GC003252.
- Hart, S. R. (1984), A large-scale isotope anomaly in the Southern Hemisphere mantle, *Nature*, **309**, 753–757, doi:10.1038/309753a0.
- Hart, S. R., E. H. Hauri, L. A. Oschmann, and J. A. Whitehead (1992), Mantle plumes and entrainment: Isotopic evidence, *Science*, **256**(5056), 517–520, doi:10.1126/science.256.5056.517.
- Hauff, F., K. Hoernle, and A. Schmidt (2003), Sr–Nd–Pb composition of Mesozoic Pacific oceanic crust (Site 1149 and 801, ODP Leg 185): Implications for alteration of ocean crust and the input into the Izu–Bonin–Mariana subduction system, *Geochim. Geophys. Geosyst.*, **4**(8), 8913, doi:10.1029/2002GC000421.
- Hawkesworth, C. J., M. S. M. Mantovani, P. N. Taylor, and Z. Palacz (1986), Evidence from the Parana of south Brazil for a continental contribution to Dupal basalts, *Nature*, **322**(6077), 356–359, doi:10.1038/322356a0.

- Heezen, B. C., et al. (1973), 5. Northwest Pacific Basaltic Basement: DSDP Site 197, *Initial Rep. Deep Sea Drill. Proj.*, 20, 43–49, doi:10.2973/dsdp.proc.20.105.1973.
- Heydolph, K., D. T. Murphy, J. Geldmacher, I. V. Romanova, A. Greene, K. Hoernle, D. Weis, and J. Mahoney (2014), Plume versus plate origin for the Shatsky Rise oceanic plateau (NW Pacific): Insights from Nd, Pb and Hf isotopes, *Lithos*, 200–201, 49–63, doi:10.1016/j.lithos.2014.03.031.
- Hickey-Vargas, R., J. M. Hergt, and P. Spandra (1995), The Indian Ocean-type isotopic signature in Western Pacific marginal basins: Origin and significance, in *Active Margins and Marginal Basins of the Western Pacific*, *Geophys. Monogr. Ser.* 88, edited by B. Taylor and J. Natland, pp. 175–197, AGU, Washington, D. C., doi:10.1029/GM088p0175.
- Hickey-Vargas, R., I. P. Savov, M. Bisimis, T. Ishii, and K. Fujioka (2006), Origin of diverse geochemical signatures in igneous rocks from the West Philippine Basin: Implications for tectonic models, in *Back-Arc Spreading Systems: Geological, Biological, Chemical and Physical Interactions*, edited by D. M. Christie, pp. 287–303, AGU, Washington, D. C.
- Hirahara, Y., Q. Chang, T. Miyazaki, T. Takahashi, R. Senda, and J.-I. Kimura (2012), Improved Nd chemical separation technique for $^{143}\text{Nd}/^{144}\text{Nd}$ analysis in geological samples using packed Ln resin columns, *JAMSTEC Rep. Res. Dev.*, 15, 25–31.
- Hirahara, Y., J.-I. Kimura, R. Senda, T. Miyazaki, T. Takahashi, H. Kawabata, Q. Chang, V. S. Bogdan, T. Sato, and S. Kodaira (2015), Geochemical variations in Japan Sea back-arc basin basalts formed by high-temperature adiabatic melting of mantle metasomatized by sediment subduction components, *Geochem. Geophys. Geosyst.*, 16, 1324–1347, doi:10.1002/2015GC005720.
- Hirano, N., et al. (2006), Volcanism in response to plate flexure, *Science*, 313, 1426–1428, doi:10.1126/science.1128235.
- Hoernle, K., F. Hauff, R. Werner, P. van den Bogaard, A. D. Gibbons, S. Conrad, and R. D. Muller (2011), Origin of Indian Ocean Seamount Province by shallow recycling of continental lithosphere, *Nat. Geosci.*, 4, 883–887, doi:10.1038/ngeo1331.
- Hofmann, A. W. (2003), Sampling mantle heterogeneity through oceanic basalts: Isotopes and trace elements, in *Treatise on Geochemistry, The Mantle and Core*, edited by R. E. Carlson, pp. 61–101, Elsevier, London, U. K.
- Hofmann, A. W., and S. R. Hart (2007), Another nail in which coffin?, *Science*, 315(5808), 39–40, doi:10.1126/science.315.5808.39c.
- Huang, S., M. Regelous, T. Thordarson, and F. A. Frey (2005), Petrogenesis of lavas from Detroit Seamount: Geochemical differences between Emperor Chain and Hawaiian volcanoes, *Geochem. Geophys. Geosyst.*, 6, Q01L06, doi:10.1029/2004GC000756.
- Ishizuka, O., M. Yuasa, R. N. Taylor, and I. Sakamoto (2009), Two contrasting magmatic types coexist after the cessation of back-arc spreading, *Chem. Geol.*, 266, 274–296, doi:10.1016/j.chemgeo.2009.06.014.
- Ito, G., and J. J. Mahoney (2005), Flow and melting of a heterogeneous mantle: 2. Implications for a chemically nonlayered mantle, *Earth Planet. Sci. Lett.*, 230, 47–63, doi:10.1016/j.epsl.2004.10.034.
- Iwamori, H., F. Albarède, and H. Nakamura (2010), Global structure of mantle isotopic heterogeneity and its implications for mantle differentiation and convection, *Earth Planet. Sci. Lett.*, 299, 339–351, doi:10.1016/j.epsl.2010.09.014.
- Janney, P. E., and P. R. Castillo (1997), Geochemistry of Mesozoic Pacific mid-ocean ridge basalt: Constraints on melt generation and the evolution of the Pacific upper mantle, *J. Geophys. Res.*, 102, 5207–5229, doi:10.1029/96JB03810.
- Jochum, K. P., U. Nohl, K. Herwig, E. Lammel, B. Stoll, and A. W. Hofmann (2005), GeoReM: A new geochemical database for reference materials and isotopic standards, *Geostand. Geoanal. Res.*, 29, 333–338, doi:10.1111/j.1751-908X.2005.tb00904.x.
- Kanazawa, T., et al. (2001), 4. Site 1179, *Proc. Ocean Drill. Program Initial Rep.*, 191, 1–159, doi:10.2973/odp.proc.ir.191.104.2001.
- Kelley, K. A., T. Plank, J. N. Ludden, and H. Staudigel (2003), Composition of altered oceanic crust at ODP Sites 801 and 1149, *Geochem. Geophys. Geosyst.*, 4(6), 8910, doi:10.1029/2002GC000435.
- Kempton, P. D., J. A. Pearce, T. L. Barry, F. J.G., C. H. Langmuir, and D. M. Christie (2002), Sr-Nd-Pb-Hf isotope results from ODP Leg 187: Evidence for mantle dynamics of the Australian-Antarctic Discordance and origin of the Indian MORB source, *Geochem. Geophys. Geosyst.*, 3(12), 1074, doi:10.1029/2002GC000320.
- Kiminami, K., N. Kashiwagi, and S. Miyashita (1992), Occurrence and significance of in-situ greenstones from the Mugai formation in the Upper Cretaceous Shimanto Supergroup, eastern Shikoku, Japan, *J. Geol. Soc. Jpn.*, 98, 867–883.
- Kiminami, K., S. Miyashita, and K. Kawabata (1994), Ridge collision and in situ greenstones in accretionary complexes: An example from the Late Cretaceous Ryukyu Islands and southwest Japan margin, *Island Arc*, 3, 103–111, doi:10.1111/j.1440-1738.1994.tb00098.x.
- Kimura, J.-I., and H. Kawabata (2014), Trace element mass balance in hydrous adiabatic mantle melting: The Hydrous Adiabatic Mantle Melting Simulator version 1 (HAMMS1), *Geochem. Geophys. Geosyst.*, 15, 2467–2493, doi:10.1002/2014GC005333.
- Kimura, J.-I., and H. Kawabata (2015), Ocean Basalt Simulator version 1 (OBS1): Trace element mass balance in adiabatic melting of a pyroxenite-bearing peridotite, *Geochem. Geophys. Geosyst.*, 15, 267–300, doi:10.1002/2014GC005606.
- Kimura, J.-I., and J. Nakajima (2014), Behaviour of subducted water and its role in magma genesis in the NE Japan arc: A combined geochemical and geochemical approach, *Geochim. Cosmochim. Acta*, 143, 165–188, doi:10.1016/j.gca.2014.1004.1019.
- Kimura, J.-I., and T. Yoshida (2006), Contributions of slab fluid, mantle wedge and crust to the origin of Quaternary lavas in the NE Japan arc, *J. Petrol.*, 47, 2185–2232.
- Kimura, J.-I., R. J. Stern, and T. Yoshida (2005), Reinitiation of subduction and magmatic responses in SW Japan during Neogene time, *Geol. Soc. Am. Bull.*, 117, 969–986, doi:10.1130/B25565.1.
- Kimura, J.-I., T. W. Sisson, N. Nakano, M. L. Coombs, and P. Lipman (2006), Isotope geochemistry of early Kilauea magmas from the submarine Hilina bench: The nature of the Hilina mantle component, *J. Volcanol. Geotherm. Res.*, 151, 51–72.
- Kimura, J.-I., J. R. K. Adam, M. Rowe, N. Nakano, M. Katakuse, P. van Keken, B. Hacker, and R. J. Stern (2010), Origin of cross-chain geochemical variation in Quaternary lavas from northern Izu arc: A quantitative mass balance approach on source identification and mantle wedge processes, *Geochem. Geophys. Geosyst.*, 11, Q10011, doi:10.1029/2010GC003050.
- Kimura, J.-I., et al. (2014), Diverse magmatic effects of subducting a hot slab in SW Japan: Results from forward modeling, *Geochem. Geophys. Geosyst.*, 15, 691–739, doi:10.1002/2013GC005132.
- Klein, E. M., C. H. Langmuir, A. Zindler, H. Staudigel, and R. Hamelin (1988), Isotopic evidence of a mantle convection boundary at the Australian-Antarctic Discordance, *Nature*, 333, 623–629, doi:10.1038/333623a0.
- Konter, J. G., B. B. Hanan, J. Blichert-Toft, A. A. P. Koppers, T. Plank, and H. Staudigel (2008), One hundred million years of mantle geochemical history suggest the retiring of mantle plumes is premature, *Earth Planet. Sci. Lett.*, 275(3–4), 285–295, doi:10.1016/j.epsl.2008.08.023.
- Koppers, A. A. P., H. Staudigel, M. S. Pringle, and J. R. Wijbrans (2003), Short-lived and discontinuous intraplate volcanism in the South Pacific: Hot spots or extensional volcanism?, *Geochem. Geophys. Geosyst.*, 4(10), 1089, doi:10.1029/2003GC000533.
- Kuritani, T., E. Ohtani, and J.-I. Kimura (2011), Intensive hydration of the mantle transition zone beneath China caused by ancient slab stagnation, *Nat. Geosci.*, 4, 713–716.
- Kuritani, T., J.-I. Kimura, E. Ohtani, H. Miyamoto, and K. Furuyama (2013), Transition zone origin of potassic basalts from Wudalianchi volcano, northeast China, *Lithos*, 156–159, 1–12, doi:10.1016/j.lithos.2012.10.010.

- Kuritani, T., T. Yoshida, J.-I. Kimura, T. Takahashi, Y. Hirahara, T. Miyazaki, R. Senda, Q. Chang, and Y. Ito (2014), Primary melt from Sannomegata volcano, NE Japan arc: Constraints on generation conditions of rear-arc magmas, *Contrib. Mineral. Petrol.*, *167*, doi:10.1007/s00410-014-0969-7.
- Li, Y.-B., et al. (2013), High-Mg Adakite and Low-Ca Boninite from a Bonin Fore-arc Seamount: Implications for the Reaction between Slab Melts and Depleted Mantle, *J. Petrol.*, *54*, 1149–1175, doi:10.1093/ptrology/egt008.
- Machida, S., N. Hirano, and J.-I. Kimura (2009), Evidence for recycled plate material in Pacific upper mantle unrelated to plumes, *Geochim. Cosmochim. Acta*, *73*, 3028–3037, doi:10.1016/j.gca.2009.01.026.
- Macpherson, G. C., and R. Hall (2001), Tectonic setting of Eocene boninite magmatism in the Izu–Bonin–Mariana forearc, *Earth Planet. Sci. Lett.*, *186*, 215–230, doi:10.1016/S0012-821X(01)00248-5.
- Mahoney, J. J., R. Frei, M. L. G. Tejada, X. X. Mo, P. T. Leat, and T. F. Nägler (1998), Tracing the Indian Ocean mantle domain through time: Isotopic results from old west Indian, east Tethyan, and south Pacific seafloor, *J. Petrol.*, *39*, 1285–1306, doi:10.1093/ptroj/39.7.1285.
- Mahoney, J. J., R. A. Duncan, M. L. G. Tejada, W. W. Sager, and B. T. J. (2005), Jurassic-Cretaceous boundary age and mid-ocean-ridge-type mantle source for Shatsky Rise, *Geology*, *33*, 185–188, doi:10.1130/G21378.1.
- Martynov, Y. A., J.-I. Kimura, A. Y. Martynov, A. V. Rybin, and M. Katakuse (2012), Indian MORB-type mantle beneath the Kuril island arc: Isotopic investigation of the mafic lavas of Kunashir Island, *Petrology*, *20*, 102–110, doi:10.1134/S0869591111060026.
- McDonough, W. F., and C. Chauvel (1991), Sample contamination explains the Pb isotopic composition of some Rurutu island and Sasha seamount basalts, *Earth Planet. Sci. Lett.*, *105*, 397–404, doi:10.1016/0012-821X(91)90180-P.
- Miyazaki, T., et al. (2012), Development of a fully automated open column chemical separation system -COLUMNSPIDER- and its application to Sr-Nd-Pb isotope analyses of igneous rock samples, *J. Mineral. Petrol. Sci.*, *107*, 74–78.
- Müller, R. D., M. Sdrolias, C. Gaina, B. Steinberger, and C. Heine (2008), Long-term sea-level fluctuations driven by ocean basin dynamics, *Science*, *319*, 1357–1362, doi:10.1126/science.1151540.
- Münker, C., S. Weyer, E. Scherer, and K. Mezger (2001), Separation of high field strength elements (Nb, Ta, Zr, Hf) and Lu from rock samples for MC-ICPMS measurements, *Geochem. Geophys. Geosyst.*, *2*(12), 1064, doi:10.1029/2001GC000183.
- Nakanishi, M., K. Tamaki, and K. Kobayashi (1989), Mesozoic magnetic anomaly lineations and seafloor spreading history of the northwestern Pacific, *J. Geophys. Res.*, *94*, 15,437–15,462, doi:10.1029/JB094iB11p15437.
- National Oceanic and Atmospheric Administration (2000), ETOPO5 5-minute gridded elevation data. [Available at <http://www.ngdc.noaa.gov/mgg/global/etopo5.HTML>]
- Nebel, O., C. Münker, Y. J. Nebel-Jacobsen, T. Kleine, K. Mezger, and N. Mortimer (2007), Hf–Nd–Pb isotope evidence from Permian arc rocks for the long-term presence of the Indian–Pacific mantle boundary in the SW Pacific, *Earth Planet. Sci. Lett.*, *254*(3–4), 377–392, doi:10.1016/j.epsl.2006.11.046.
- Nohda, S. (2009), Formation of the Japan Sea basin: Reassessment from Ar–Ar ages and Nd–Sr isotopic data of basement basalts of the Japan Sea and adjacent regions, *J. Asian Earth Sci.*, *34*, 599–609, doi:10.1016/j.jseae.2008.08.003.
- Okamura, S., R. J. Arculus, and Y. A. Martynov (2005), Cenozoic magmatism of the north-eastern Eurasian margin: The role of lithosphere versus asthenosphere, *J. Petrol.*, *46*, 221–253, doi:10.1093/ptrology/egh065.
- Park, S. H., S. M. Lee, and R. J. Arculus (2006), Geochemistry of basalt from the Ayu Trough, equatorial western Pacific, *Earth Planet. Sci. Lett.*, *248*(3–4), 700–714, doi:10.1016/j.epsl.2006.06.021.
- Pearce, J. A. (2008), Geochemical fingerprinting of oceanic basalts with applications to ophiolite classification and the search for Archean oceanic crust, *Lithos*, *100*, 14–48, doi:10.1016/j.lithos.2007.06.016.
- Pearce, J. A., and I. J. Parkinson (1993), Trace element models for mantle melting: Application to volcanic arc petrogenesis., in *Magmatic Processes and Plate Tectonics*, edited by H. M. Prichard et al., pp. 373–403, Geol. Soc. Spec. Publ., London, U. K.
- Pearce, J. A., P. D. Kempton, G. M. Nowell, and S. R. Noble (1999), Hf–Nd element and isotope perspective on the nature and provenance of mantle and subduction components in western Pacific arc-basin systems, *J. Petrol.*, *40*, 1579–1611, doi:10.1093/ptroj/40.11.1579.
- Pearce, J. A., P. D. Kempton, and J. B. Gill (2007), Hf–Nd evidence for the origin and distribution of mantle domains in the SW Pacific, *Earth Planet. Sci. Lett.*, *260*, 98–114, doi:10.1016/j.epsl.2007.05.023.
- Plank, T. (2005), Constraints from Thorium/Lanthanum on sediment recycling at subduction zones and the evolution of the continents, *J. Petrol.*, *46*, 921–944, doi:10.1093/ptrology/egi005.
- Plank, T., and C. H. Langmuir (1998), The chemical composition of subducting sediment and its consequences for the crust and mantle, *Chem. Geol.*, *145*, 325–394, doi:10.1016/S0009-2541(97)00150-2.
- Plank, T., K. A. Kelley, R. W. Murray, and L. Q. Stern (2007), Chemical composition of sediments subducting at the Izu–Bonin trench, *Geochem. Geophys. Geosyst.*, *8*, Q04116, doi:10.1029/2006GC001444.
- Poulet, A., J.-S. Lee, P. Vidal, B. Cousens, and H. Bellon (1995), Cretaceous to Cenozoic volcanism in South Korea and in the Sea of Japan: Magmatic constraints on the opening of the back-arc basin., in *Volcanism Associated With Extension at Consuming Plate Margins*, edited by J. L. Smellie, pp. 169–191, Geol. Soc. Spec. Publ., London, U. K.
- Pyle, D., D. M. Christie, J. J. Mahoney, and R. A. Duncan (1995), Geochemistry and geochronology of ancient southeast Indian and southwest Pacific seafloor, *J. Geophys. Res.*, *100*, 22,261–22,282, doi:10.1029/95JB01424.
- Reagan, M. K., et al. (2010), Fore-arc basalts and subduction initiation in the Izu–Bonin–Mariana system, *Geochem. Geophys. Geosyst.*, *11*, Q03X12, doi:10.1029/2009GC002871.
- Rehkamper, M., and A. W. Hofmann (1997), Recycled ocean crust and sediment in Indian Ocean MORB, *Earth Planet. Sci. Lett.*, *147*(1–4), 93–106, doi:10.1016/S0012-821X(97)00009-5.
- Roger, L. L., R. Moberly, D. Bukry, H. P. Foreman, J. V. Gardner, J. B. Keene, Y. Lancelot, H. Luterbacher, M. C. Marshall, and A. Matter (1975a), 2. Site 303: Japanese magnetic lineations, *Initial Rep. Deep Sea Drill. Proj.*, *32*, 17–43, doi:10.2973/dsdp.proc.32.102.1975.
- Roger, L. L., R. Moberly, D. Bukry, H. P. Foreman, J. V. Gardner, J. B. Keene, Y. Lancelot, H. Luterbacher, M. C. Marshall, and A. Matter (1975b), 3. Site 304: Japanese magnetic lineations, *Initial Rep. Deep Sea Drill. Proj.*, *32*, 45–73, doi:10.2973/dsdp.proc.32.103.1975.
- Saito, M., S. Murakami, and M. Ogasawara (2007), Establishment of stratigraphic framework of the Shimanto accretionary complex in Yakushima Island, Japan, based on newly found Eocene radiolarian fossils, *J. Geol. Soc. Jpn.*, *113*, 266–269.
- Sakuyama, T., et al. (2013), Melting of dehydrated oceanic crust from the stagnant slab and of the hydrated mantle transition zone: Constraints from Cenozoic alkaline basalts in eastern China, *Chem. Geol.*, *359*, 32–48, doi:10.1016/j.chemgeo.2013.09.012.
- Sakuyama, T., S. Nagaoka, T. Miyazaki, Q. Chang, T. Takahashi, Y. Hirahara, R. Senda, T. Itaya, J.-I. Kimura, and K. Ozawa (2014), Melting of the uppermost metasomatized asthenosphere triggered by fluid fluxing from ancient subducted sediment: Constraints from the Quaternary basalt lavas at Chugaryeong volcano, Korea, *J. Petrol.*, *55*, 499–528, doi:10.1093/ptrology/egt074.
- Sano, S., and Y. Hayasaka (2004), Sr and Nd isotope geochemistry of Hole1179D basalts, in *Proc. Ocean Drill. Program Sci. Results*, edited by W. W. Sager, T. Kanazawa and C. Escutia, pp. 1–11.

- Sano, T., K. Shimizu, A. Ishikawa, R. Senda, Q. Chang, J.-I. Kimura, M. Widdowson, and W. W. Sager (2012), Variety and origin of magmas on Shatsky Rise, northwest Pacific Ocean, *Geochem. Geophys. Geosyst.*, *13*, Q08010, doi:10.1029/2012GC004235.
- Savov, I. P., R. Hickey-Vargas, M. D'Antonio, J. G. Ryan, and P. Spadea (2006), Petrology and geochemistry of West Philippine Basin basalts and early Palau–Kyushu arc volcanic clasts from ODP Leg 195, Site 1201D: Implications for the early history of the Izu–Bonin–Mariana arc, *J. Petrol.*, *47*(2), 277–299, doi:10.1093/petrology/egi075.
- Sdrolas, M., and R. D. Müller (2006), Controls on back-arc basin formation, *Geochem. Geophys. Geosyst.*, *7*, Q04016, doi:10.1029/2005GC001090.
- Seton, M., et al. (2012), Global continental and ocean basin reconstructions since 200 Ma, *Earth Sci. Rev.*, *113*(3–4), 212–270, doi:10.1016/j.earscirev.2012.03.002.
- Seton, M., N. Flament, J. Whittaker, R. D. Müller, M. Gurnis, and D. J. Bower (2015), Ridge subduction sparked reorganization of the Pacific plate-mantle system 60–50 million years ago, *Geophys. Res. Lett.*, *42*, 1732–1740, doi:10.1002/2015GL063057.
- Shimoda, G., O. Ishzuka, K. Yamashita, M. Yoshitake, M. Ogasawara, and M. Yuasa (2011), Tectonic influence on chemical composition of ocean island basalts in the West and South Pacific: Implication for a deep mantle origin, *Geochem. Geophys. Geosyst.*, *12*, Q07020, doi:10.1029/2011GC003531.
- Staudigel, H., K.-H. Park, M. S. Pringle, J. L. Rubenstone, W. H. F. Smith, and A. Zindler (1991), The longevity of the South Pacific isotope and thermal anomaly, *Earth Planet. Sci. Lett.*, *102*, 24–44, doi:10.1016/0012-821X(91)90015-A.
- Stixrude, L., and C. Lithgow-Bergelloni (2012), Geophysics of chemical heterogeneity in the mantle, *Annu. Rev. Earth Planet. Sci.*, *40*, 569–595, doi:10.1146/annurev.earth.36.031207.124244.
- Stracke, A., M. Bizimis, and V. J. M. Salters (2003), Recycling oceanic crust: Quantitative constraints, *Geochem. Geophys. Geosyst.*, *4*(3), 8003, doi:10.1029/2001GC000223.
- Stracke, A., A. W. Hofmann, and S. R. Hart (2005), FOZO, HIMU, and the rest of the mantle zoo, *Geochem. Geophys. Geosyst.*, *6*, Q05007, doi:10.1029/2004GC000824.
- Straub, S. M., S. L. Goldstein, C. Class, and A. Schmidt (2009), Mid-ocean-ridge basalt of Indian type in the northwest Pacific Ocean basin, *Nat. Geosci.*, *2*, 286–289, doi:10.1038/ngeo471.
- Straub, S. M., S. L. Goldstein, C. Class, A. Schmidt, and A. Gomez-Tuena (2010), Slab and mantle controls on the Sr–Nd–Pb–Hf isotope evolution of the post 42 Ma Izu–Bonin Volcanic Arc, *J. Petrol.*, *51*, 993–1026, doi:10.1093/petrology/egq009.
- Straub, S. M., J. D. Woodhead, and R. J. Arculus (2015), Temporal evolution of the Mariana Arc: Mantle wedge and subducted slab controls revealed with a tephra perspective, *J. Petrol.*, *56*, 409–439, doi:10.1093/petrology/egv005.
- Sun, S.-s., and W. F. McDonough (1989), Chemical and isotopic systematics of oceanic basalts: Implications for mantle composition and processes, in *Magmatism in the Ocean Basins*, edited by A. D. Saunders and M. J. Norry, pp. 313–345, Geol. Soc. Spec. Publ., London, U. K.
- Taira, A. (2001), Tectonic evolution of the Japanese island arc system, *Annu. Rev. Earth Planet. Sci.*, *29*, 109–134, doi:10.1146/annurev.earth.29.1.109.
- Takahashi, T., Y. Hirahara, T. Miyazaki, B. S. Vaglarov, Q. Chang, J.-I. Kimura, and Y. Tatsumi (2009), Precise determination of Sr isotope ratios in igneous rock samples and application to micro-analysis of plagioclase phenocrysts, *JAMSTEC Rep. Res. Dev.*, 59–64.
- Tollstrup, D., J. B. Gill, A. J. R. Kent, D. Prinkey, R. Williams, Y. Tamura, and O. Ishizuka (2010), Across-arc geochemical trends in the Izu–Bonin arc: Contributions from the subducting slab, revisited, *Geochem. Geophys. Geosyst.*, *11*, Q01X10, doi:10.1029/2009GC002847.
- United State Geological Survey (2000), Global 30 Arc-Second Elevation (GTOPO30). [Available at <https://lta.cr.usgs.gov/GTOPO30>.]
- Wessel, P., and W. H. F. Smith (1998), New, improved version of the Generic Mapping Tools released, *Eos Trans. AGU*, *79*, 579, doi:10.1029/98EO00426.
- Whittaker, J. M., R. D. Müller, G. Leitchenkov, H. Stagg, M. Sdrolas, C. Gaina, and A. Goncharov (2007), Major Australian–Antarctic Plate Reorganization at Hawaiian–Emperor Bend Time, *Science*, *318*, 83–86, doi:10.1126/science.1143769.
- Willbold, M., and A. Stracke (2006), Trace element composition of mantle end-members: Implications for recycling of oceanic and upper and lower continental crust, *Geochem. Geophys. Geosyst.*, *4*, Q04004, doi:10.1029/2005GC001005.
- Woodhead, J. D., R. J. Stern, J. Pearce, J. Hergt, and J. Vervoort (2012), Hf–Nd isotope variation in Mariana Trough basalts: The importance of “ambient mantle” in the interpretation of subduction zone magmas, *Geology*, *40*, 539–542, doi:10.1130/g32963.1.
- Zhang, J., and Y. Nozaki (1996), Rare earth elements and yttrium in seawater: ICP–MS determinations in the East Caroline, Coral Sea, and South Fiji basins of the western South Pacific Ocean, *Geochim. Cosmochim. Acta*, *60*, 4631–4644, doi:10.1016/S0016-7037(96)00276-1.
- Zhao, D., Y. Tian, J. Lei, L. Liu, and S. Zheng (2009), Seismic image and origin of the Changbai intraplate volcano in East Asia: Role of big mantle wedge above the stagnant Pacific slab, *Phys. Earth Planet. Inter.*, *173*, 197–206.
- Zindler, A., and S. R. Hart (1986), Chemical geodynamics, *Annu. Rev. Earth Planet. Sci.*, *14*, 493–571.